E-164X

High Gradient Plasma-Wakefield Acceleration Using Ultrashort Electron Bunches

C.E. Barnes, C. O'Connell, F.J. Decker, P. Emma, M.J. Hogan, R. Iverson, P. Krejcik, R.H. Siemann, and D. Walz*
Stanford Linear Accelerator Center
C. E. Clayton, C. Huang, D. K. Johnson, C. Joshi, W. Lu, K. A. Marsh, and W. B. Mori*
University of California, Los Angeles
S. Deng, T. Katsouleas, P. Muggli and E. Oz*
University of Southern California

Abstract

This is a proposal to extend the E-164 plasma wakefield accelerator (PWFA) experiment from 100 μm down to 20 μm long electron bunches. Such short bunches will be available in the SLAC Final Focus Test Beam (FFTB) in the near future. Numerical simulations show that peak accelerating gradients on the order of 15 GeV/m can be driven by 20 μm long bunches with $1x10^{10}$ electrons in a plasma with a density in the 10^{17} cm^{-3} range. For this experiment we will choose the plasma length such that the total energy gain or gradient-length product will remain within the energy acceptance of the FFTB dumpline. This work will test the validity of the PWFA in a new physical regime, and will lay the ground work for a possible "plasma afterburner" or energy doubler operating at extremely high accelerating gradients. The experiment will also be the first to operate in the regime where the bunch length, bunch radius and plasma wavelength are all of the same order, and as such will be a valuable data point where no scaling laws exist for the PWFA.

I. Introduction

For the past four years, the E-157 and E-162 collaborations have been studying key issues related to the applicability of plasmas to future high-energy accelerators [1]. In particular we have been examining the beam-driven plasma wakefield accelerator [2] (PWFA) scheme and electron and positron focusing by plasmas[3] in the context of an e^+-e^- linear collider. This is because plasmas can provide accelerating gradients and focusing

forces that are orders of magnitude greater than those obtained using more conventional technology.

The E-157 experiment [4] studied the transverse and longitudinal electron beam propagation issues in a 1.4 meter-long plasma that would act as a prototype accelerating stage for an eventual PWFA. Experiment E-162 [5] continued the acceleration work with electrons after making several key improvements to the experimental apparatus. These improvements were made possible by relocating the plasma chamber 12 meters upstream to the focal point of the Final Focus Test Beam (FFTB). The magnetic optics at this new location were better suited for making small spots and allowed, for the first time, the electron beam to be injected into the plasma at nearly the equilibrium or matched radius. Quadrupoles, now downstream of the plasma, were combined with the dipole magnet of the FFTB dumpline to form an imaging magnetic energy spectrometer. The latter enabled a clear differentiation of the effects related to transverse or focusing forces from the effects of energy gain and loss. E-162 also extended these measurements to positron beams. Results from E-157 and E-162 are summarized in Section VI.

Typical bunches delivered to the FFTB contained roughly 2×10^{10} electrons in a 0.6 mm long bunch. The maximum accelerating gradient for such beam parameters was of the order of 300 MeV/m. As the following paragraph will show, E-164 and E-164X will measure accelerating gradients > GeV/m. Further, the E-157/E-162 experiments have already successfully tested many of the predicted observables of a PWFA such as 1) multiple betatron oscillations of the beam as the plasma density is increased; 2) propagation of a nearly matched beam through the plasma; 3) Dynamic focusing within a single bunch 4) oscillation of the tilted beam in an ion column; 5) refraction of the beam at the plasma-neutral gas interface; 6) x-ray emission due to betatron motion in the ion column; 7) focusing of a positron beam; 8) acceleration and de-aceleration of an electron drive beam; and 9) acceleration and de-acceleration of a positron drive beam.

Beginning in April 2003, E-164 [6] will revisit the original goal: ultrahigh gradient plasma-wakefield acceleration. Ultrahigh gradient, in this context, refers to peak acceleration gradients of > 1 GeV/m. It was possible to contemplate such an experiment because of the availability of shorter electron bunches in the near future at the FFTB, where the experiments are carried out. We expect the Ultrashort Bunch Facility [7]

(USBF) to deliver σ_z = 100 μm bunches compared to σ_z = 600 μm bunches used in E-157/E-162. Since in the linear theory the accelerating gradient scales as the beam charge divided by the bunch length squared, a factor of six reduction in pulse length translates to a factor of 36 increase in the accelerating gradient.

The ultrahigh gradients generated by a 20μm bunch are comparable to those achieved with short pulse laser beams in plasmas. However, since an electron beam can be self-guided by the ion channel and its natural diffraction length is typically longer than the Rayleigh length of a focused laser beam, the gradient times length product is typically much greater in the electron beam case leading to a larger energy gain per stage.

However, a shorter electron bunch requires a higher plasma density source. With a 30 cm long plasma source at the optimum plasma electron density of 5.6 x 10^{15} cm^{-3}, numerical simulations predict that particles in the tail will gain an average energy of 1.75 GeV with some particles gaining as much as 4.4 GeV. The imaging spectrometer developed by the E-162 collaboration is absolutely necessary for making these measurements. With a vertical energy dispersion of 300 MeV/mm a total energy gain of up to 3 GeV can be measured while staying within the energy acceptance of the FFTB dumpline. For E-164 we therefore need to reduce the length of the plasma source to about 30 cm in order to be able to safely transport a total energy change of up to 2.5 GeV (loss of 0.7 GeV and gain of 1.8 GeV) as the bunch length is decreased to 0.1 mm. For E-164X the plasma density needs to be increased to above 10^{17} cm^{-3}, and keeping the total bunch energy spread less than 3 GeV will necessitate shortening the plasma still further to a few cm in length. It should be noted that producing plasmas of the appropriate density, length and radial extent for these experiments is non-trivial and discussed further in Section VI.

The PWFA has been proposed as a possible energy doubler for a linear collider, where a "plasma afterburner" is used in conjunction with an ultra-relativistic beam from a more conventional linac [1, Appendix A]. While E-164 will be the first experiment to utilize the compressed bunches, the purpose of this proposal is to suggest using the ultimate performance of the USBF to demonstrate the extraordinary accelerating gradients required for a plasma afterburner. Since it is a natural extension to E-164, in this document we call this experiment E-164X. It will take advantage of the unique capabilities afforded in the remaining lifetime of the FFTB. What we propose, is in

essence a continuation of the work on shorter bunches and higher gradients that will begin with E-164. We will take advantage of the fully compressed bunch (assumed to be less than 20μm r.m.s.) to drive a plasma wakefield accelerator with peak accelerating gradients in excess of 10 GeV/m. To operate such an experiment within the current energy acceptance of the FFTB, we will make the plasma length correspondingly shorter, such that the gradient-length product still produces a beam within the energy acceptance of the FFTB. Such an experiment will also be the first to operate in the regime where the bunch length, bunch radius and plasma wavelength are all of the same order, and as such will be a valuable data point where no scaling laws exist for the PWFA.

The most ambitious follow-on experiment will involve a plasma on the order of one meter in length and accelerating gradients >10 GeV/m. However, the large induced energy spread (O(100%)) would necessitate significant costs for both additional magnets and shielding. In light of the limited lifetime of the FFTB, such an experiment may not be practical at this time. However, successful completion of E-164 and E-164X will provide strong motivation to add a new beamline, the so-called FFTB2 with the capability to do the complete experiment and double the energy of a significant fraction of the drive electron beam within a few meters.

We believe that the successful demonstration of these experiments will be a truly significant and defining accomplishment in the Advanced Accelerator Research and High Energy Density fields [8, Appendix B]. Since the short pulse capability will be available at the FFTB for only a short period of time, the proposed ultrahigh gradient plasma wakefield acceleration experiments represent a window of opportunity that cannot be missed. The E-164/E-164X collaboration has the proven ability (see Section VI) and expertise to conduct these experiments. Most of the experiment and diagnostics (see Section III) are already in place as part of the upcoming E-164 experiment. The experimental work will be carried out in conjunction with theory and simulations programs that are absolutely necessary for the success of the experiments.

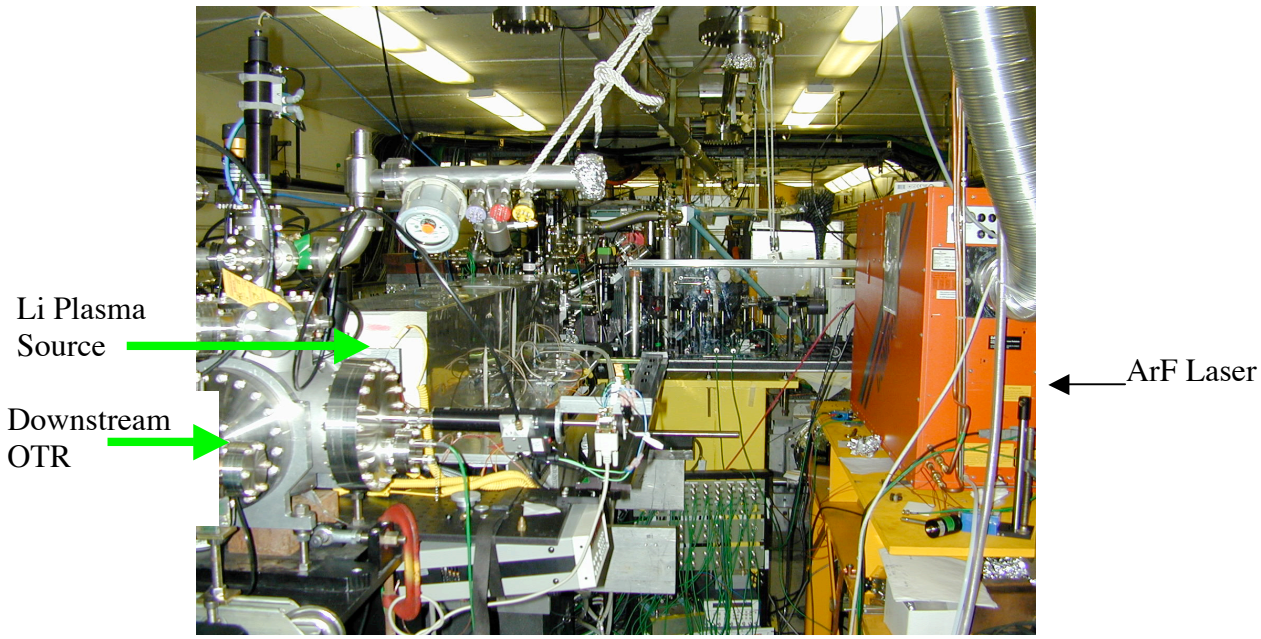

Figure 1. Existing E-162 experimental apparatus at IP-0 in the FFTB.

We begin by defining the symbols used throughout this proposal.

Table 1: Legend of symbols used in this proposal

Physical Parameter	**Symbol**
Speed of Light in Vacuum	c
Charge of an Electron	e
Classical Electron Radius	$e^2/4\pi\varepsilon_0 m_e c^2$
Accelerating Gradient	eE
Plasma Focusing Gradient	$K=\omega_p/(2\gamma)^{1/2}c$
Plasma Wavenumber	$k_p=\omega_p/c$
Plasma Wavelength	$\lambda_p=2\pi/k_p$
Mass of an Electron	m_e
Number of electrons per Bunch	N
Drive Beam Density	$n_b=N/(2\pi)^{3/2}\sigma_r^2\sigma_z$
Plasma Density	n_p
Drive Beam Transverse Size	σ_r
Drive Beam Bunch Length	σ_z
Beam Plasma Frequency	$\omega_{pb}=(n_b e^2/\varepsilon_b m_e)$
Electron Plasma Frequency	$\omega_p=(n_o e^2/\varepsilon_b m_e)$
Beta Function of the Beam	β
Normalized Emittance of the Beam	$\gamma\varepsilon$ = $\gamma\varepsilon$
Spot Size of the Beam in x, y	σ_x, σ_y
Focal Length of the Lens in x, y	f_x, f_y
Skin Depth of Plasma	c/ω_p

II. Motivation and Method

In the beam-driven plasma wakefield accelerator (PWFA), a short but high current electron bunch, with beam density n_b larger than the plasma electron density n_p, expels the plasma electrons [9] as shown in Fig. 2. If the length of the bunch is approximately half the wavelength of the relativistic plasma wave ($k_p\sigma_z \approx \sqrt{2}$), then the expelled plasma electrons rush back in and set-up a large plasma wakefield which has a phase velocity that is exactly the beam velocity ≈ c. According to linear plasma theory the wake amplitude is [10]

$$eE_{linear}[eV/cm] = \sqrt{n_0}\,\frac{n_b}{n_0}\,\frac{\sqrt{2\pi}k_p\sigma_z e^{-\frac{k_p^2\sigma_z^2}{2}}}{1+\frac{1}{k_p^2\sigma_r^2}} \qquad (1)$$

For $k_p\sigma_r << 1$, this is optimized for $k_p\sigma_z \approx \sqrt{2}$ with a value given by

$$eE_{linear} = 240\,MeV/m\left[\frac{N}{4\times10^{10}}\right]\left[\frac{0.6}{\sigma_z(mm)}\right]^2 \qquad (2)$$

where N is the number of particles in the electron bunch and σ_z is the bunch length.

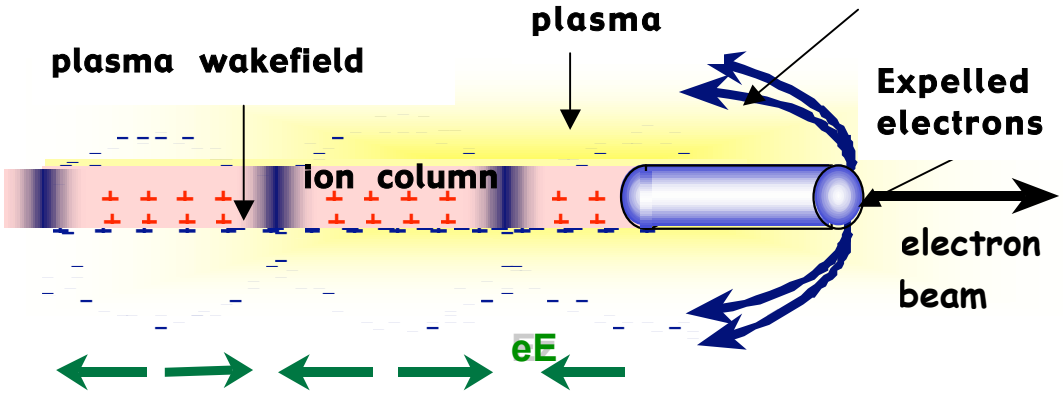

Figure 2. Physical mechanism of the Plasma Wakefield Accelerator.

In E-157, E-162 and E-164 the wake is excited in the so called blow-out regime ($n_b > n_p$ and $k_p\sigma_r << 1$) where the wake excitation is highly nonlinear. However, 3D PIC code simulations have borne out this $1/\sigma_z^2$ linear theory scaling of the peak accelerating

gradient. For beam and plasma parameters of interest the accelerating field is highly non-linear (spikey) and with a peak value

$$(eE)_{peak} \approx 3 \text{ to } 4 (eE)_{linear}$$

and the useful portion (see Fig. 3) of the wake is somewhere in between the peak value and the absolute value given by linear theory $(eE)_{linear}$.

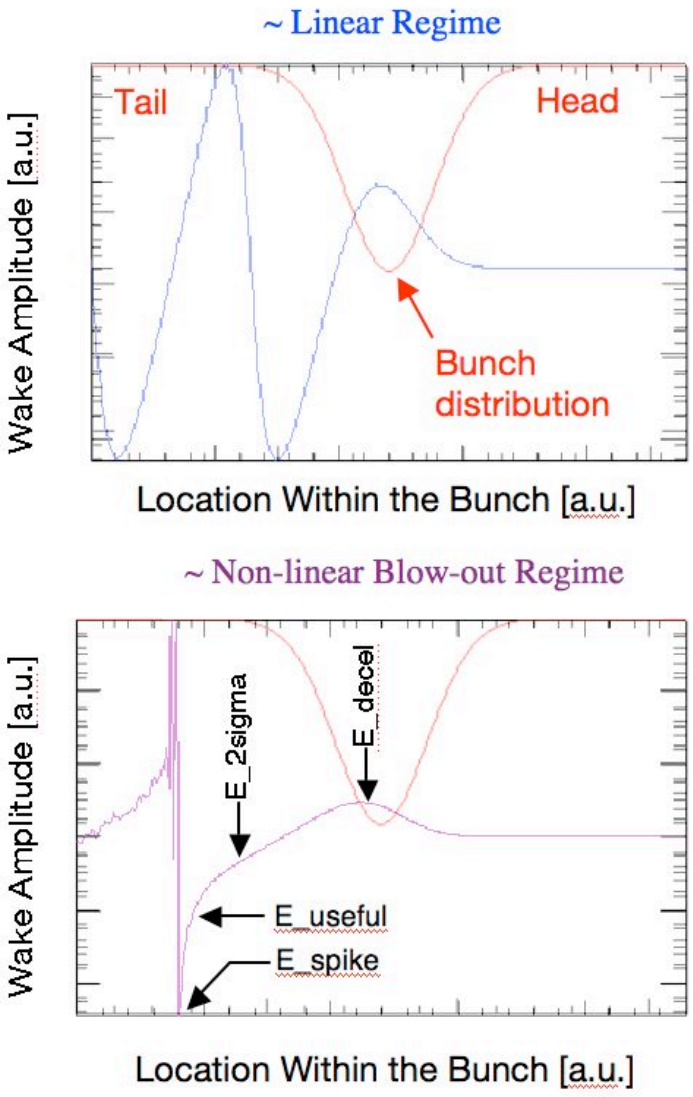

Figure 3: The longitudinal wakefield is shown for a nearly linear case (top) and a non-linear blow-out case (bottom). Arrows indicate various locations within the wake referred to in the curves in Fig. 4. Note that in the non-linear blow-out case the peak accelerating field is 10x larger than the nearly linear case. Also note that the peak accelerating field occurs later in the bunch for the more non-linear case.

Experiments E-164 and E-164X are designed to test the bunch length scaling of the accelerating gradient in the PWFA. The scaling of this useful portion of the wake deviates from the $1/\sigma_z^2$ scaling for bunches so short that σ_r/σ_z is no longer << 1 or when $k_p\sigma_r \sim 1$ (recall $k_p = \sqrt{2}/\sigma_z$). This is new territory the PWFA experiments where E-164X will operate. In E-164X, $k_p\sigma_r \sim 1$, so the wake may not be excited in the blow-out regime, but $n_b/n_0 > 1$ so the wake may still be non-linear.

With the USBF the bunch length in the FFTB will be reduced from the present 600 μm to 100 μm, and eventually down to less than 20 μm. The wide range of parameters explored by these experiments can be appreciated immediately by comparing the existing and proposed parameters available to the FFTB shown in Table 2.

Table 2: Comparison of the Current (E-162) and Proposed (E-164, E-164X) Short-Pulse Beam Parameters

	Current Beam	**E-164**	**E-164X**
N	2×10^{10}	$1\text{-}2 \times 10^{10}$	1×10^{10}
σ_z(mm)	0.6-0.7	0.1-0.15	0.01-0.02
σ_r(μm)	10-50	20-40	< 25
$\Delta E/E$(r.m.s.)	0.4%	0.6%	1.5%
I_{peak}	1-3 kA	10-20 kA	50-100 kA
β_x	50 m	50 m	50 μm
β_y	5 m	5 m	5 μm

As mentioned before, for $n_b >> n_p$ the linear plasma theory is not valid. We have developed extensive computer simulation capabilities that allow us to perform one-to-one modeling of the experiment in this highly non-linear regime. The code used, OSIRIS [9] is a 3-D, fully electromagnetic, relativistic, parallelized particle-in-cell (PIC) code that has been benchmarked against other codes and model problems that can be solved numerically. OSIRIS is now the standard tool for simulating the beam plasma interactions in E-162/E-164 and E-164X and has successfully predicted many of the observed phenomena in a quantitative manner.

To understand the non-linear wakefields that will be produced by the wide range of beam parameters given in Table 2, a series of OSIRIS simulations have been performed where the bunch length was varied from 650μm down to 20μm, for a fixed bunch charge *N* with the plasma density varied to maintain $k_p\sigma_z = \sqrt{2}$. The magnitude of

the accelerating and de-accelerating field, for various locations within the bunch, is plotted versus bunch length in Figure 4.

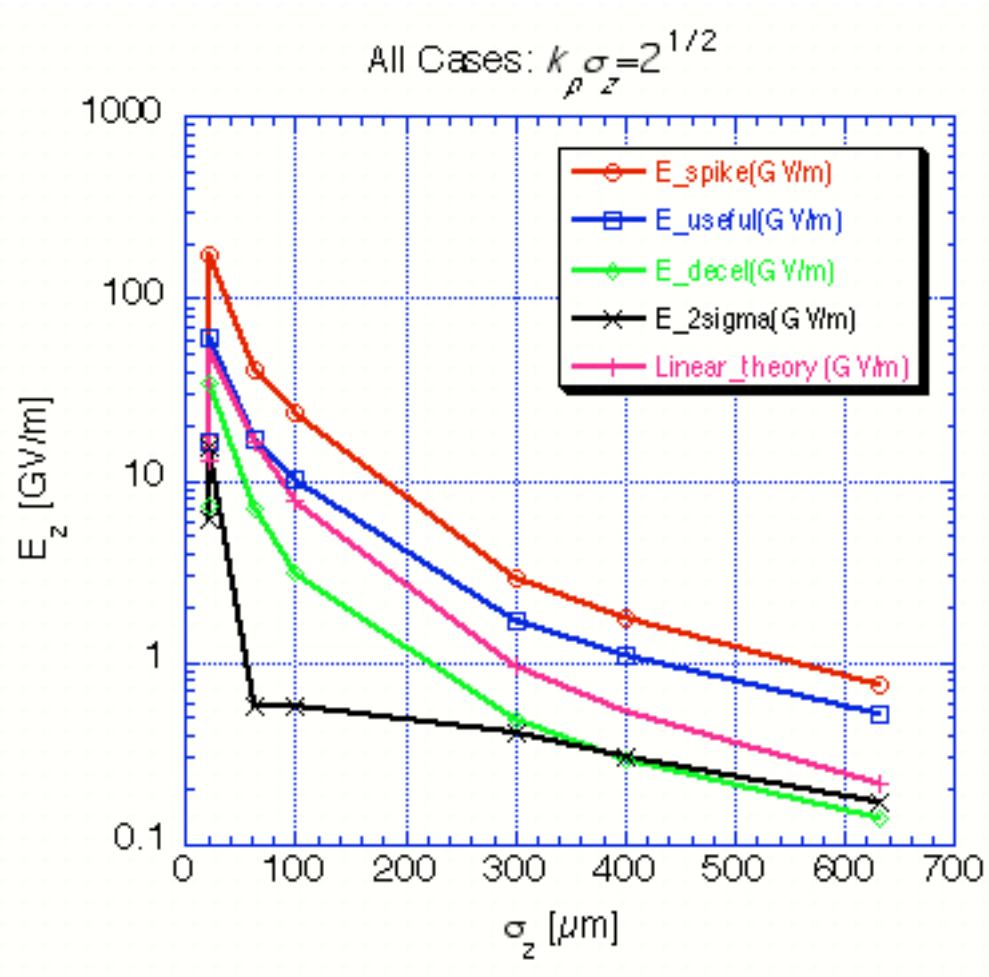

Figure 4. OSIRIS simulations of the accelerating field at various locations within the bunch, as well as the scaling predicted by the linear theory, are plotted vs. the bunch length. Note all simulation points are for N=4x10^{10} except for the σ_z=20μm case where there are points for both N=1x10^{10} and N=4x10^{10}.

Future applications of a PWFA will beam load the wake to accelerate a large numbers of particles with a narrow energy spread. In the regime where $n_b \sim n_p$ and where the linear theory is valid, the beam loading can be understood as the superposition of the wake from the driving bunch (or portion of a single bunch) and the wake of the witness bunch (or portion of a single bunch) [11]. No theory for the beam loading of non-linear wakes in a PWFA exists. It is therefore important to understand the nature of the

wakes from these short bunches not only from the standpoint of driving large amplitude plasma wakes, but also in preparing for the future when extremely short bunches will be used to beam load the wakes and produce an accelerated witness bunch with a narrow energy spread.

As in E-164, there are other experiments that can be carried out as part of this work. One critical experiment involves the continued testing for the growth of the electron-hose instability. The ability to propagate short bunches stably without breakup due to the hosing instability [12] is critical to the future application of this method of acceleration as a possible afterburner to a linear collider. The increase in the displacement of the centroid of the beam can be measured as a function of plasma density to determine the extent of the hosing growth. No significant growth has been measured up to $2x10^{14}$ e^-/cm^3 over 1.4 m.

Another aspect of E-164X will extend the previous work in E-157 on betatron produced x-rays (see Section VI). It has been estimated that a significant fraction of the electrons in the bunch will undergo such betatron motion (due to the focusing force of the ion column) as to radiate at photon energies well above the electron-positron pair production threshold. Conversion of the betatron gamma rays to positrons in target of a high-Z material will offer a proof of principle test of the applicability of this technique to positron production for a linear collider. By extracting some of the electron beam energy in a plasma as photons and doing the pair production in a separate converter target, as opposed to a more conventional solid positron target (where both processes take place in the same volume), this technique offers greater mechanical robustness. This idea is explored further in Appendix C.

III. Existing Experimental Apparatus

Figure 5 shows the schematic of the experimental set up for E-164. The FFTB beam traverses two, 25 μm thick titanium Optical Transition Radiation (OTR) foils before and after going through the plasma source placed at IP-0. The OTR foils allow monitoring of the electron beam profile and give information needed to tune out any beam tails.

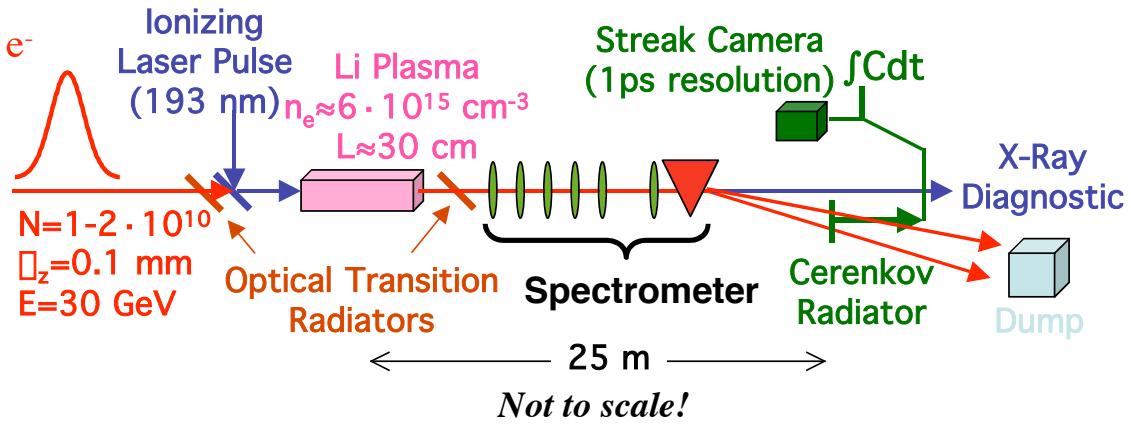

Figure 5. Schematic of the experimental set-up used for the E-164 experiment.

The quadruples downstream of IP-0, in conjunction with the FFTB dipole dump magnet form a magnetic imaging energy spectrometer. After exiting the spectrometer the beam traverses an aerogel Cherenkov emitter. The Cherenkov radiation is image relayed to the outside of the FFTB bunker where it is time resolved in both planes. Quadrupoles after the aerogel will be used to control the beam divergence en route to the beam dump. In addition to these diagnostics the beam position is monitored throughout the FFTB by a series of beam position monitors and beam charge is monitored with toroids.

Data is acquired by shot-by-shot correlations. The upstream and downstream OTR images, the time integrated Cherenkov image, the two (x vs. t) and (y vs. t) streak camera images and laser and beam data are acquired on each shot and information from these diagnostics can be combined for filtering and sorting of data. It should be noted that as the bunch length is decreased to 100μm and below, this will be below the temporal resolution of the streak camera and we will use changes to the overall energy spread as the primary energy gain diagnostic. This does not pose a problem for E-164 and E-164X as the energy changes resulting from the PWFA mechanism (~3%) will now be larger than the incoming beam energy spread (~1.5%).

IV. Experimental Issues For E-164X

Although the experimental arrangement for the proposed E-164X experiment is similar to that for E-164 there are some crucial differences:

1) Producing and Measuring Bunches < 50μm in Length:

The bunch length will be maximally compressed to 50μm by the chicane in Sector 10 of the linac. The additional correlated energy spread induced by longitudinal wakefields in the remaining 2km of linac will be used, in conjunction with the R_{56} in the FFTB, to compress the beam further to a predicted r.m.s. length of 12μm. Bunch lengths down to 50μm can be measured using the newly commissioned transverse deflecting cavity [13] in Sector 29, but as yet there are no diagnostics in place that can measure the sub 50μm bunches in the FFTB. The Short Pulse Photon Science (SPPS) group is actively pursuing electro-optical techniques capable of such measurements, and preliminary design work has been completed. We plan to take advantage of the expertise they develop for tuning and measuring beam properties in this regime.

2) The Ratio σ_r/σ_z:

Using shorter bunches is attractive so long as the wake amplitude scales with $1/\sigma_z^2$, but there are other important issues to consider when going to ever shorter bunches. First, the "blow-out" regime is defined by $n_b > n_p$ and $k_p\sigma_r << 1$. If the optimum wake occurs for $k_p\sigma_z \approx \sqrt{2}$, then n_b/n_p is proportional to σ_z/σ_r^2. To maintain $n_b/n_p >> 1$ with shorter bunches requires the beam to be focused ever smaller. For bunches with $\sigma_z < 20$ μm it will be difficult to maintain $n_b/n_p > 1$ without reducing σ_r well below the 25μm typical of E-162. If $\sigma_r > \sigma_z$ we will be in a PWFA regime not yet significantly explored where the gradients are lower than for $\sigma_r < \sigma_z$.

The second issue to consider is the blow-out time, σ_{blow}, relative to the bunch length ($\sigma_b=\sigma_z/c$). For stable propagation and low emittance growth we need $\sigma_{blow} < \sigma_b$. If the ion channel forms slowly, then each slice along the beam will experience a different focusing force, or worse, all the plasma electrons will not leave the channel during the pulse and the wake amplitude will be reduced. For $n_b/n_p > 1$, the blow-out time is approximately $\sigma_{blow} \approx \sqrt{2}/\omega_b$, where ω_b is the beam plasma frequency. The ratio σ_b/σ_{blow} then scales as $\sqrt{\sigma_z/\sigma_r}$. Even for 100 μm bunches, if the incoming beam size σ_r is on the order of 25μm the blow-out time might be too slow for our purposes and the blow-out issue needs to be explored further.

The effects of all these issues will be minimized or negated completely if σ_r can be made sufficiently small. For E-164, with 100μm long bunches and an r.m.s. energy spread of 0.6%, simulations indicate that with typical SLC normalized emittances of 50 x 5 mm-mrad, a round beam of σ_r = 13μm is achievable. For E-164X the r.m.s. energy spread will increase to 1.5% for the maximally compressed pulse of 12μm giving a spot size of 17μm at the plasma entrance. These values have been calculated based on the locations of the upstream beryllium window and titanium OTR foil, which increase the beam emittance through multiple Coulomb scattering. Optimization of the locations of various elements is ongoing, but we expect the spots sizes listed above will be an upper bound rather than a lower limit.

3) Producing and Measuring Plasmas with $n_pL > 10^{17}$ cm^{-2}:

From the linear theory, the optimum density for a given bunch length is given by $k_p\sigma_z = 2$ and so $n_p \sim 1/\sigma_z^2$. This imposes a major challenge for the plasma source to increase the density from that used in E-162 by a factor of 36 for E-164 and another factor of 25 for E-164X. It can be shown that the plasma density length product (n_pL) is proportional to the laser fluence, w (Joules/ cm^2) when using UV single photon ionization to produce the plasma. This will allow us to increase the plasma density as we go to shorter bunches, but at the expense of the plasma length. The optimal gradient depends only on the bunch length and charge according to the relation, Gradient~N/σ_z^2 where N is the beam charge. As stated above, n_pL is fixed by the laser fluence ($n_pL \sim w$). Therefore, the bunch length fixes n_p, and L is not a free parameter. The total energy gain is, (Gradient)(L) ~$(N/\sigma_z^2)L \sim Nw$. The implication is that while the accelerating gradient increases as the bunch length gets shorter, the total energy gain is the same and fixed by the laser fluence and the beam charge only (for single photon ionized plasmas).

We plan to have a plasma source where we can trade plasma density for plasma length and thus make adjustments for whatever bunch length is used. With our present E-164 design we have $n_pL \approx 2\text{x}10^{17}$ cm^{-2} and L=30 to 40 cm. If we want to change from 100 μm bunches to 20 μm bunches, the density will have to go up ~25 and the plasma length will go down ~25.

For short bunches and $n_pL > 2\text{x}10^{17}$ cm^{-2}, using laser ionization to produce the plasma might be impractical. We will use tunnel ionization as a method to reach very

large plasma density-length products. As the electron bunch is made shorter to increase the accelerating gradient of the PWFA module, its radial space charge field also increases. For a bunch with a Gaussian profile in *r* and *z*, the maximum electric field is given by $E_{r\,max}(GV/m) \approx 5.2 \times 10^{-19} N/\sigma_r\sigma_z$, where *N* is the number of particles in the bunch, and σ_r and σ_z are the bunch rms sizes. This field is reached in the middle of the bunch (z=0), and at $r \approx 1.6\sigma_r$. This field can exceed the threshold for field-, or tunnel-ionization of the vapor in which the bunch propagates. The threshold for field-ionization depends on the vapor ionization potential ϕ and is of the order of 4.4 GV/m for cesium (ϕ=3.9 eV) and 6.8 GV/m for lithium (ϕ=5.4 eV). With short bunches the threshold can be exceeded over a large enough volume that the self-ionized plasma is similar to a pre-ionized plasma for the wake excitation. The fractional ionization created by a σ_r=15 μm, σ_z=20 μm bunch with $N=10^{10}$ electrons is shown in Fig. 6. The ionization process is essentially a threshold process, and therefore full ionization of the vapor's first electron is reached up to $\approx 2\sigma_z$ ahead of the bunch, and up to ≈ 110 μm radially. For such a short bunch the optimum plasma density for wake excitation, as given by the linear theory, is $\approx 3.9 \times 10^{17} cm^{-3}$, and the plasma electrons are expelled to a radius smaller than the plasma radius. The wake amplitude driven in an infinite pre-ionized plasma can thus be expected in this case. Since the transverse focusing force of the plasma wake allows for the channeling of the electron bunch over many beam beta functions, meters-long, self-ionized PWFA modules could lead to large energy gain in single high-gradient PWFA modules. The self-ionization process could suppress the need for staging of PWFA modules to achieve large energy gains.

In the self-ionized regime, the plasma density is adjusted through the vapor density, which is very stable in a heat-pipe oven, and is insensitive to shot-to-shot changes of the beam parameters. Figure 7 shows the vapor curve of cesium and lithium. Higher neutral vapor densities, and therefore plasma densities, are achieved at lower temperatures in cesium than in lithium, and cesium is also easier to ionize than lithium (lower ϕ). However, lithium has a much larger ionization potential for its second electron (75.6 eV, ionization threshold of 293 GV/m) than cesium (23.21 eV, ionization threshold of 61 GV/m), which helps to prevent contribution to the plasma density from the ionization of the second electron.

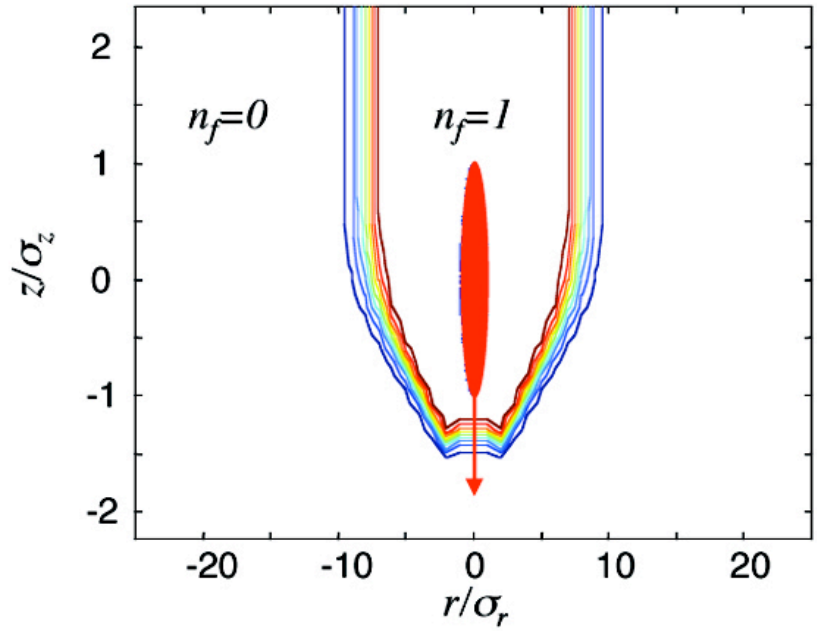

Figure 6: Fractional ionization n_f in the (r,z) plane created by a bunch with σ_z=20 μm, σ_r=15 μm, and N=10^{10} particles in Cs. The ionization fraction n_f is 0 far from the beam and reaches 1 around and behind the beam. The beam is propagating in the direction of the arrow, and contours are plotted by n_f steps of 0.1. The r=σ_r contour of the beam is also shown.

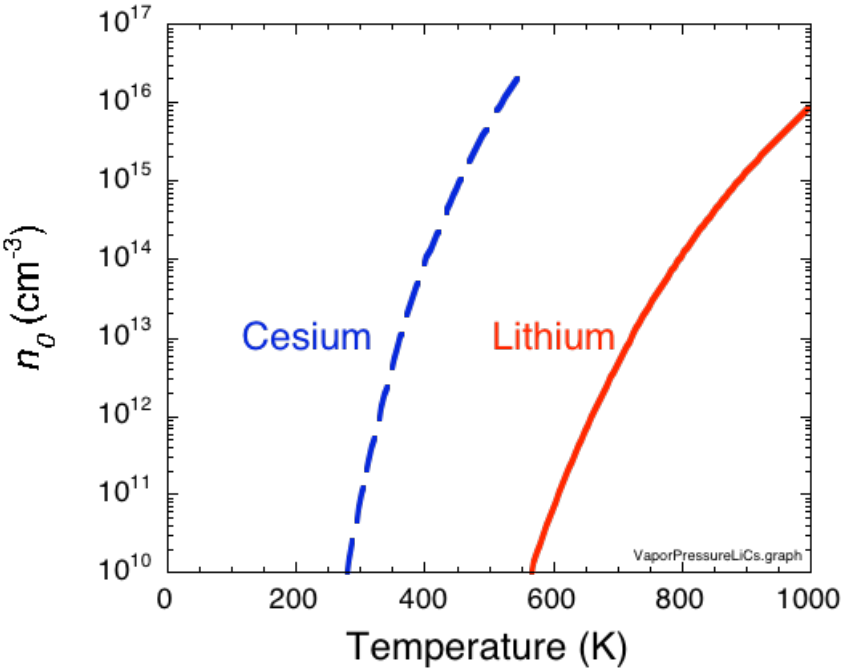

Figure 7: Vapor curves for cesium and lithium. The buffer gas in a heat-pipe oven would be He(Z=2), for Li(Z=3), and Xe(Z=54) or Ar(Z=18) for Cs(Z=55). Neutral densities appropriate for short bunches are achieved at lower temperatures with Cs than Li.

V. Experimental Program Schedule

This is an ambitious and difficult experiment. It can only be carried out after it is demonstrated that sub-20μm bunches can be delivered at IP-0 with parameters stated in Table. 2. Assuming that this will be realized by the end of the E-164 and SPPS runs in 2003, we would like to request additional experimental time consisting of two four week blocks of time followed by eight to ten weeks of time in between for analysis and iteration.

VI. Results from E-157/E-162 Experiments

E-157 experiment called, " One GeV Beam Acceleration in a One Meter Long Plasma Cell," was proposed in 1997, began running in the summer of 1998 and concluded data taking in the Spring of 2000. It was a truly pioneering experiment as there had never been any work done on the interaction of GeV class electron bunches with plasmas. The experiment yielded an enormous amount of data and several papers (See Section VIII) have either been published or submitted.

Experiment E-162 called, "Positron and Electron Dynamics in a Plasma Wakefield Accelerator" was approved in the Winter of 2000. It had a very successful first run that demonstrated dynamic focusing of a 28.5 GeV positron beam and a second run on electron acceleration in the PWFA that was completed at the end of July 2001. The final E-162 run used these same techniques to explore energy loss and gain in a positron beam driven PWFA. The data from these runs is still being analyzed, but several papers are in preparation for submission.

We describe below highlights of some of the results that have been obtained by the E-157/E-162 collaborations.

1) ***Focusing of Positron Beams by an Extended Plasma Column:***

Time-integrated and time-resolved measurements of the focusing of a 28 GeV positron beam as it traverses a 1.4 m long plasma column have been made. The beam size at two different locations downstream of the plasma as a function of plasma density has been measured over a wide range of plasma densities. A maximum demagnification of greater than 2 has been demonstrated.

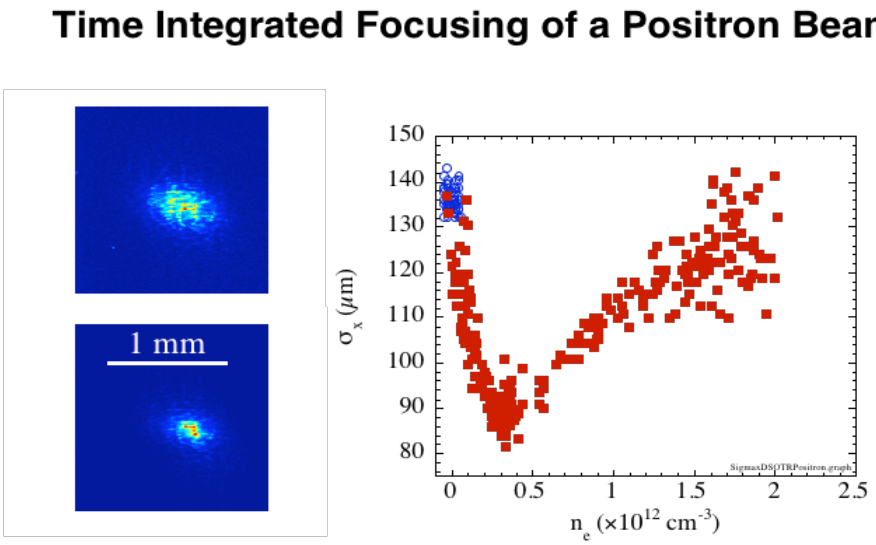

Figure 8. Time integrated images on the downstream OTR with (bottom left) and without (upper left) the plasma indicating positron beam focusing and spot size variation on the downstream OTR as a function of plasma density.

2) ***Propagation of Matched and Unmatched Beams Through An Ion Column:***

We have shown that when the beam is matched to the plasma ($\beta_{beam} = \beta_{plasma}$) it propagates through it without significant oscillations of its beam envelope over a wide range of densities. This matched propagation also minimizes the oscillation of the beam tail thereby reducing the transverse momentum imparted to the particles in the beam tail. When the beam is not matched, the beam can undergo multiple betatron oscillations of its envelope within the plasma. Experimentally, these oscillations are observable as an oscillation of the spot size of the beam on a screen downstream of the plasma as the plasma density is increased.

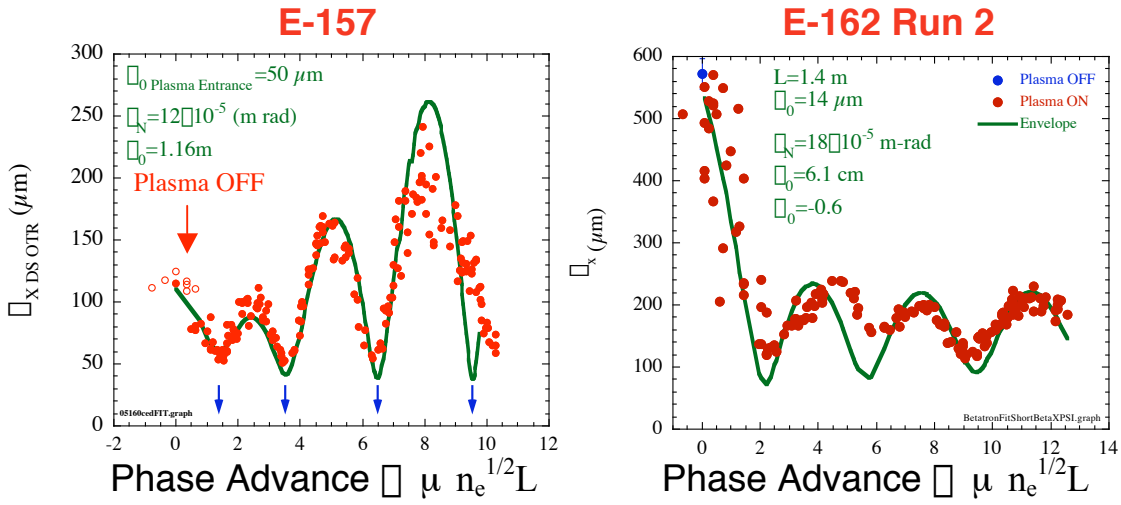

Figure 9: Oscillations of the beam envelope observed on the downstream OTR due to betatron motion of the electrons in experiment E-157 (left) and E-162 (right). The beam in E-157 was larger than the matched size resulting in the growth in the envelope oscillation, while the beam was nearly matched in E-162 resulting in no growth in the beam envelope oscillations.

3) ***Dynamic Focusing Within a Single Bunch:***

In the blow-out regime, as the beam propagates through the plasma, the density of plasma electrons along the incoming bunch drops from the ambient density to zero leaving a pure ion channel for the bulk of the beam.

Thus, from the head of the beam up to the point where all plasma electrons are blown out, each successive longitudinal slice of the bunch experiences an increasing focusing force due to the plasma ions. The time-changing focusing force results in a different number of betatron oscillations for each slice depending upon its location within the bunch. Since the incoming electron beam has a correlated energy spread, this time-dependent focusing of the electron bunch has been observed by measuring the beam spot size at the Cherenkov radiator, which is in the image plane of a magnetic energy-spectrometer imaging the plasma exit. Each plot in Fig. 10 represents a section in time, where time progresses from left to right, then top to bottom. We see in Fig. 10 that the number of betatron oscillations within the bunch increases towards the back of the bunch (Figs. 10a–10g) but only up to the blowout time occurring approximately at the plot labeled ξ = 0 psec (Fig. 10h). Clearly, each successive slice of the bunch, from ξ = -4.9 psec to ξ = 0, is experiencing a stronger effective focusing force than the slice prior to it. Conversely, the ambient plasma density needed to reach any given minimum decreases with time along the bunch. The locations of the minima are both slice- and density-dependent. Figs. 10i-l are in the blow-out regime as the focusing force is no longer changing.

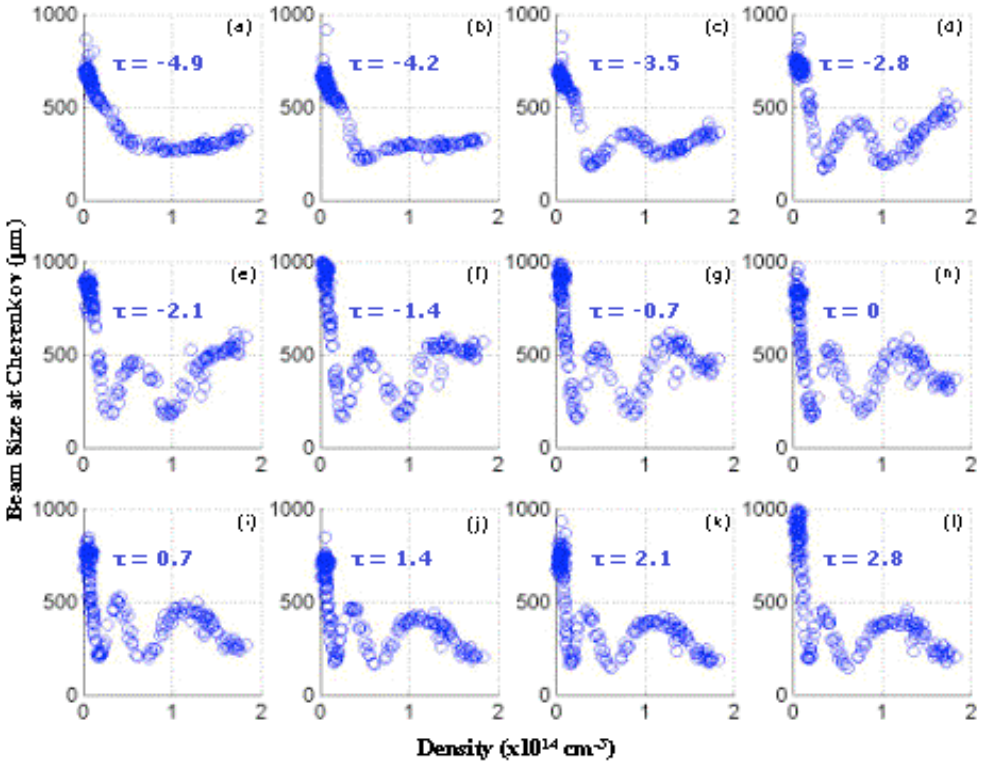

Figure 10: Individual Cherenkov Time Slices (read L-R, T-B). Graph (a) shows the weak focusing force, which dominates the first head slice. Beginning at graph (b) the slices are in the linear portion of the chirp. Graphs (i)-(l) are in the blowout regime, since the focusing force is no longer changing.

4) Experimental Test for the Electron Hosing Instability

Stable propagation of the drive bunch is essential to the operation of the PWFA. Of concern is the electron hose instability which can lead to the growth of transverse perturbations on the beam due to the nonlinear coupling of beam electrons to the plasma electrons at the edge of the ion channel through which the beam propagates. We have carried out an experiment to measure the extent of the electron hose instability by sending a beam with a known initial tilt through the plasma column. The center of mass of the beam is seen to oscillate at the betatron frequency with the maximum exit angle of the beam scaling as the square root of the plasma density as expected. No significant growth has been measured up to 2×10^{14} e^-/cm^3 over 1.4 m.

5) Observation of Betatron X-ray Emission from a Plasma Wiggler

Synchrotron light sources use magnetic undulators to obtain high brightness photon beams in the x-ray region. Here we have utilized an ion channel in a plasma (instead of a magnetic wiggler/undulator) to wiggle an ultra-relativistic 28.5 GeV electron beam. The quadratic density dependence of the spontaneously emitted betatron x-ray radiation, the absolute x-ray yield at 6.4 ± 0.13 KeV of $(2 \pm 1) \times 10^7$ photons and the divergence angle of 10^{-4} radians of the forward emitted x-rays as a consequence of wiggling in the ion channel, are in good agreement with theory.

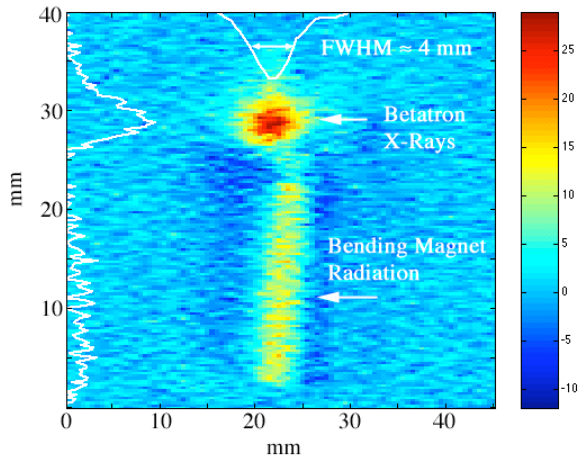

Figure 11: Betatron x-ray radiation and bending magnet radiation recorded using a fluoresor at the end of the photon beam line: E-157 experiment.

6) Refraction of the Electron Beam at a Plasma-Gas Interface

We have observed the collective refraction of a 28.5 GeV beam of electrons at a plasma/gas interface. It is orders of magnitude larger than would be expected from single electron considerations and it is unidirectional. The electron beam exiting the plasma is bent away from the normal to the plasma-neutral gas interface in analogy with light exiting a high index medium at an interface between two dielectric media.

The physical reason for this effect, observed for the first time with a particle beam, is as follows. While the beam is fully inside the plasma, the space charge at the head of the beam repels the plasma electrons out to a radius $r_c \sim (n_o/n_e)^{1/2} r_b$ where r_b is the radius of the beam, n_b is the peak density of the beam, and n_e is the plasma density. The

remaining plasma ions constitute a positive charge channel through which the latter part of the beam travels. The ions provide a net focusing force on the beam. When the beam nears the plasma boundary, the ion channel becomes asymmetric producing a deflecting force in addition to the focusing force. This asymmetric plasma lensing gives

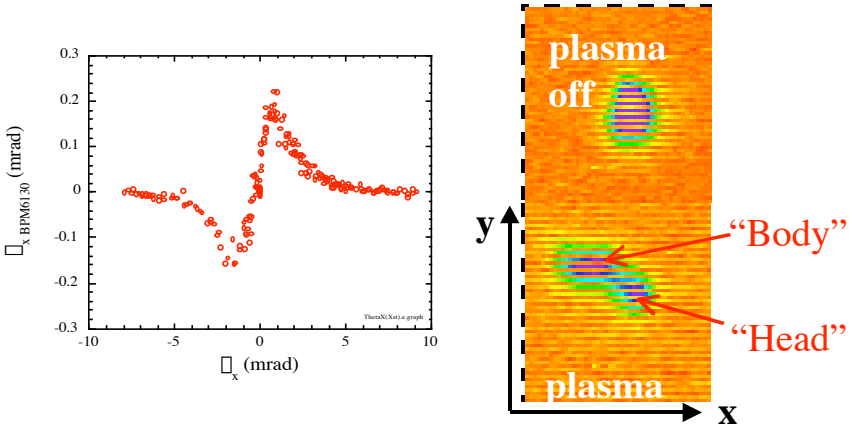

Figure 12: A plot of beam deflection ( ) measured with the beam position monitor versus angle between the laser and the beam ( ). For incident angles less than 1.2 mrad, the beam appears to be internally reflected.

rise to the bending of the beam path at the interface. The bending of the beam by the collective effect of the (passive) medium at the boundary is the particle analog to refraction of photons at a dielectric boundary.

This work was published in Nature and a more detailed version has been published in PR-STAB.

7) Electron Acceleration in a Meter Long Plasma via the Plasma Wakefield Acceleration Technique

During the second E-162 run, the E-157/E-162 set-up was moved from IP-1 to the focal point in the FFTB tunnel. An imaging spectrometer was commissioned successfully to allow imaging of the beam from the plasma exit plane to the spectrometer image plane at IP-2 which allowed for a clean separation of the transverse (focusing effects) from the longitudinal (energy loss & gain). Preliminary analysis indicates energy loss of the core and energy gain of the tail corresponding to average gradients of 110 MeV/m over 1.4 m.

The peak accelerating gradient observed is on the order of 250 MeV/m and the total number of accelerated particles in this slice is on the order of $3x10^7$.

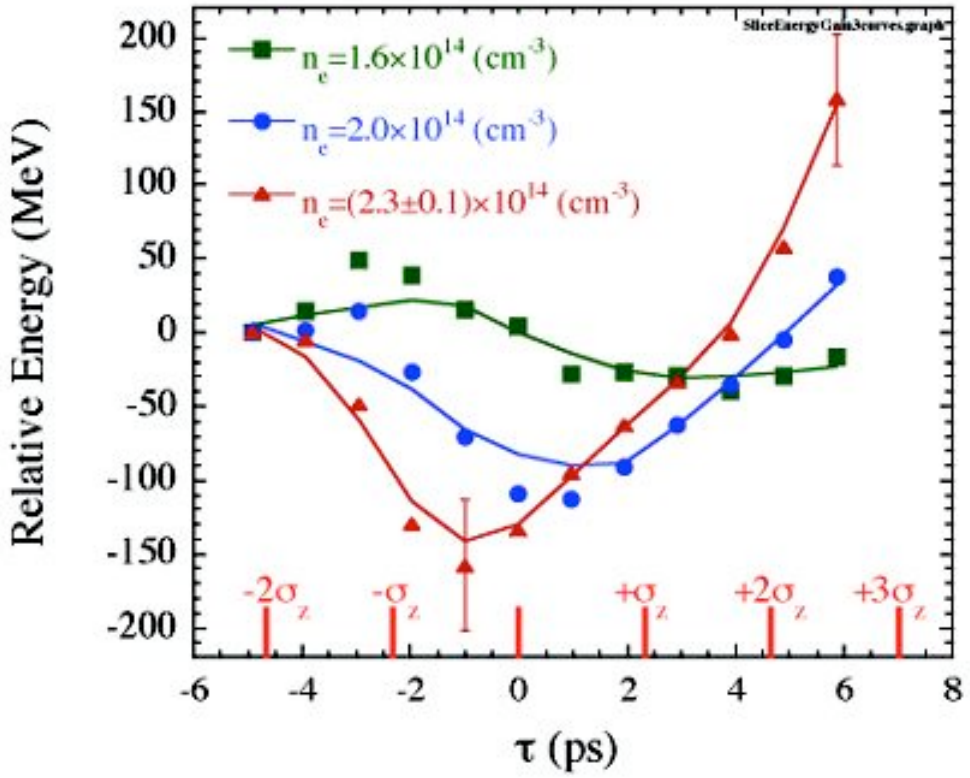

Figure 13: Preliminary measurements on the change in energy of picosecond slices of the electron beam at the resonant plasma density in E-162. De-acceleration of the core and acceleration of the tail are on the order of 110 MeV/m over 1.4 meters with peak acceleration of 250 MeV/m.

8) Positron Acceleration in a Meter Long Plasma Via the Plasma Wakefield Acceleration Technique

Critical to the application of plasma acceleration stages in future colliders is the acceleration of both electrons and positrons. Recent experimental results from E162 show the first demonstration of positron acceleration in a plasma. Figure 13 shows the energy change imparted on the 28.5 GeV positron beam after it traversed a 1.4m long plasma of density $1.8x10^{14}$ cm^{-3}. The beam's centroid lost 65±10 MeV while driving the plasma wave, and the tail of the beam $2\sigma_z$ behind the centroid, gained over 100 MeV (a gradient of over 70 MeV/m.)

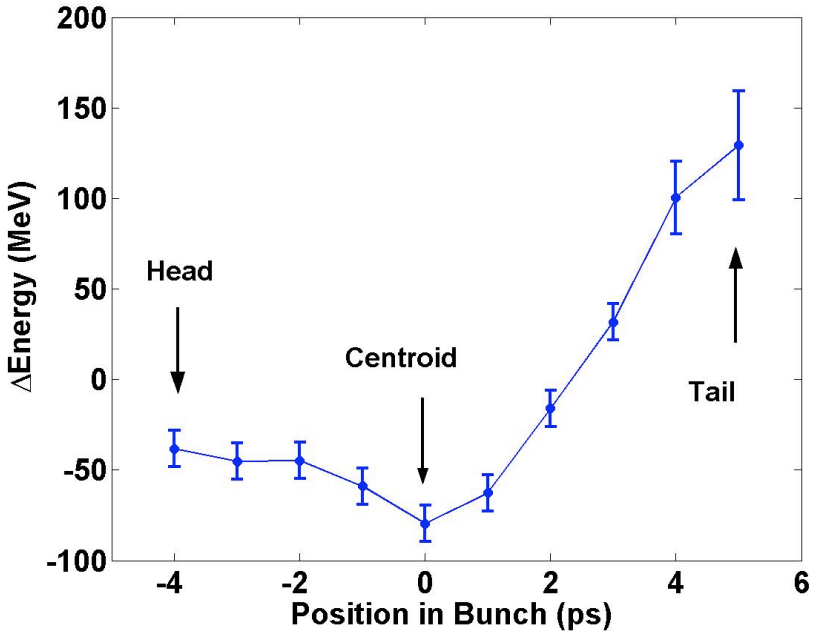

Figure 14: Preliminary analysis showing energy loss and energy gain of a positron beam after it traversed 1.4 meters of plasma in the E162 experiment

VII. Publications of the E-157/E-162 Collaboration

Peer-Reviewed Publications from E157/E162/E164

1) M. J. Hogan *et al,* "E-157: A 1.4 Meter-Long Plasma Wakefield Acceleration Experiment Using A 30 GeV Electron Beam From The Stanford Linear Accelerator Center Linac", Physics of Plasmas **7**, 2241 (2000).
2) P. Muggli *et al,* "Collective Refraction Of A Beam Of Electrons At A Plasma-Gas Interface", Nature **411**, 43 (3 May 2001)
3) P. Catravas *et al,* "Measurements Of Radiation Near An Atomic Spectral Line From The Interaction Of A 30 GeV Electron Beam And A Long Plasma", Physical Review E **64** 046502 (2001).
4) P. Muggli *et al*, "Collective Refraction Of A Beam Of Electrons At A Plasma-Gas Interface", Physical Review Special Topics - Accelerators and Beams **4**, 091301 (2001).
5) S. Lee *et al*, "Energy Doubler For A Linear Collider", Physical Review Special Topics - Accelerators and Beams **5**, 011001 (2002).
6) Shouqin Wang *et al,* "X-Ray Emission From Betatron Motion In A Plasma Wiggler", Physical Review Letters **88**, 135004 (2002)
7) C. E. Clayton *et al,* "Transverse Envelope Dynamics Of A 28.5 Gev Electron Beam In A Long Plasma", Physical Review Letters **88**, 154801 (2002)
8) C. Joshi *et al,* "High Energy Density Plasma Science With An Ultra-Relativistic Electron Beam", Physics of Plasmas **9**, 1845 (2002).
9) C. O'Connell *et al*, "Dynamic Focusing Of An Electron Beam Through A Long Plasma", submitted to Physical Review Special Topics – Accelerators and Beams

Related Peer-Reviewed Simulation Papers

1) S. Lee *et al,* "Simulations Of A Meter-Long Plasma Wakefield Accelerator", Physical Review E **61**, 7014 (2000)
2) R. G. Hemker *et al,* "Dynamic Effects In Plasma Wakefield Excitation", Physical Review Special Topics – Accelerators and Beams **3**, 061301 (2000).
3) S. Lee *et al*, "Plasma-Wakefield Acceleration Of A Positron Beam", Physical Review E **64**, 045501(R) (2001).
4) E. S. Dodd *et al*, "Hosing And Sloshing Of Short-Pulse Gev-Class Wakefield Drivers", Physical Review Letters **88**, 125001 (2002).

Papers in preparation – titles are tentative -

"Dynamics Of Ultra-Relativistic Positron-Beam Propagation In Meter-Scale Plasmas" – intended for Physical Review Letters

"Measurement Of Electron Acceleration In A Plasma Wakefield Accelerator" – intended for Science or Nature

"Plasma Wakefield Acceleration of Positrons" – intended for Physical Review Letters

More than 15 invited presentations and/or papers at conferences, workshops, universities, and laboratories.

Student Theses

1) Brent E. Blue, M.S. "Hosing Instability of the Drive Electron Beam in the E157 Plasma-Wakefield Acceleration Experiment at the Stanford Linear Accelerator" December 2000.
2) Seung Lee, Ph.D. "Non-linear Plasma Wakefield Acceleration: Models and Experiments". May 2002.
3) Sho Wang, Ph.D. "X-ray Synchrotron Radiation in a Plasma Wiggler" June 2002.

In addition, E-162, E-164 and E-164X are expected to be the focus of the PhD research of seven graduate students: Stanford (2), UCLA (3) and USC (2).

VIII. References

[1] S. Lee et al., *Phys. Rev. STAB* **5**, 011001 (2002).
[2] P. Chen et al., *Phys. Rev. Lett.* **56**, 1252 (1986).
T. Katsouleas et al., *Phys. Rev A* **33**, 2056 (1986).
J. Rosenzweig et al., *Phys. Rev. Lett.* **61**, 98 (1998).
R. Ruth et al., *Particle Accelerators* **17**, 171 (1985).
[3] P. Chen, *Particle Accelerators* **20**, 171 (1987).
J.B. Rosenzweig et al., *Phys. Rev. A* **44**, 6189 (1991).
[4] M.J. Hogan et al., *Phys. Plasmas* **7**, 2241 (2000).
[5] M.J. Hogan et al., SLAC-ARDB-242 (2000).
[6] M.J. Hogan et al., SLAC-ARDB-314 (2000).
[7] P. Emma et al., SLAC-PUB-8850 (2001).
[8] C. Joshi et al., *Phys. Plasmas* (2001).
[9] R. Hemker et al., *Phys. Rev. STAB* **3**, 061301 (2000).
[10] R. Keinigs et al., *Phys. Fluids* **30**, 252 (1987).
[11] T. Katsouleas et al., *Particle Accelerators* **22**, 81 (1987).
[12] D. Whittum et al., *Phys. Rev. Lett.* **67**, 991 (1991).
[13] R. Akre et al., SLAC-PUB-8864 (2001).

E164X Appendices

Appendix A – S. Lee *et al,* **Energy doubler for a linear collider**

Appendix B – C. Joshi *et al*, **High energy density plasma science with an ultra-relativistic electron beam**

Appendix C – C. Joshi, **Betatron Radiation Induced Positron Source For a Linear e+-e- Collider**

Energy doubler for a linear collider

S. Lee, T. Katsouleas, and P. Muggli
University of Southern California, Los Angeles, California 90089

W. B. Mori, C. Joshi, R. Hemker, E. S. Dodd, C. E. Clayton, K. A. Marsh, B. Blue, and S. Wang
University of California, Los Angeles, Los Angeles, California 90095

R. Assmann, F. J. Decker, M. Hogan, R. Iverson, and D. Walz
Stanford Linear Accelerator Center, Stanford University, Stanford, California 94309
(Received 9 August 2001; published 17 January 2002)

The concept of using short plasma sections several meters in length to double the energy of a linear collider just before the collision point is proposed and modeled. In this scenario the beams from each side of a linear collider are split into pairs of microbunches with the first driving a plasma wake that accelerates the second. The luminosity of the doubled collider is maintained by employing plasma lenses to reduce the spot size before collision.

DOI: 10.1103/PhysRevSTAB.5.011001 PACS numbers: 41.75.Lx, 52.75.–d

At 2 miles long and 50 GeV, the Stanford Linear Collider (SLC) is the highest energy linear accelerator in the world, and the only linear collider. Along with the Large Electron Positron Collider (LEP) at CERN, it has succeeded in unveiling much of the detailed physics of the standard model of elementary particles and fields. However, the Higgs boson and the ultimate test of the standard model appear now to lie above 100 GeV and therefore out of the reach of the SLC. The results of the last runs of LEP were suggestive of the fact that the discovery of the Higgs may have been just beyond the reach of that machine [1,2]. In this report, we describe a scenario for doubling the energy of a collider by using a plasma wake field accelerator section several meters long placed at the end of each beam line just before the collision point. Such a doubling scheme could be used to extend the high-energy physics reach of the SLC or a future linear collider.

The concept of a plasma wake field accelerator has received considerable attention recently [3–7]. In a plasma wake field accelerator, the space charge of a particle bunch displaces the electrons of a preformed quiescent plasma to produce a large plasma wake field that can accelerate a subsequent bunch at a very high rate. In this report, 3D simulation models are used to show that the amplitude of the accelerating wake scales with the inverse square of the bunch length and that this scaling continues to hold for parameters far exceeding the linear theory from which it is derived. This leads us to propose the concept of a plasma afterburner—a specifically designed plasma that accelerates as well as focuses each beam from a linear collider in a single, short, final stage. Finally, we outline the critical issues that remain to be addressed in order to realize this concept.

The afterburner concept is illustrated schematically in Fig. 1. Electrons and positrons are accelerated to the collider's nominal operating energy (e.g., 50 GeV for the SLC example), overcompressed to form two microbunches each, then the trailing half-bunches are doubled in energy over a few meters in the plasma afterburner. To sustain the luminosity at the interaction point (IP) at the nominal level of the original collider without the plasma, the reduction in number of particles must be offset by a smaller spot size at the IP. Reduction of the spot size is possible in the strong focusing fields of the plasma; thus, higher density plasma lenses are added to the design just before the interaction point.

To guide the discussion of the simulations to follow, we begin by reviewing key features of plasma wake field excitation in linear theory [8]. The linear response of a plasma to a Gaussian bunch is optimized when the plasma density (n_o) is chosen such that the bunch length and plasma wavelength are matched; more precisely, for $k_p \sigma_z \cong \sqrt{2}$,

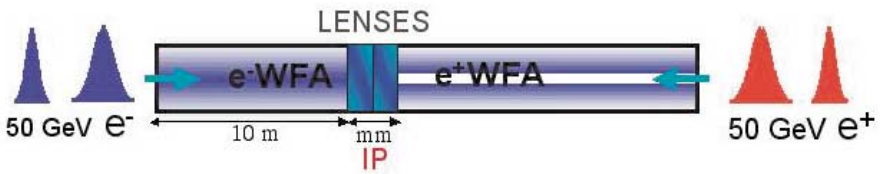

FIG. 1. (Color) Schematic of the plasma afterburner concept. Plasma wake field acceleration (WFA) sections are placed at the interaction point (IP); short plasma lens sections of higher density further focus the beams before collision. Note that the WFAs are not symmetric; the positron section may be longer to reach the same energy and may have a channel to enhance the wake.

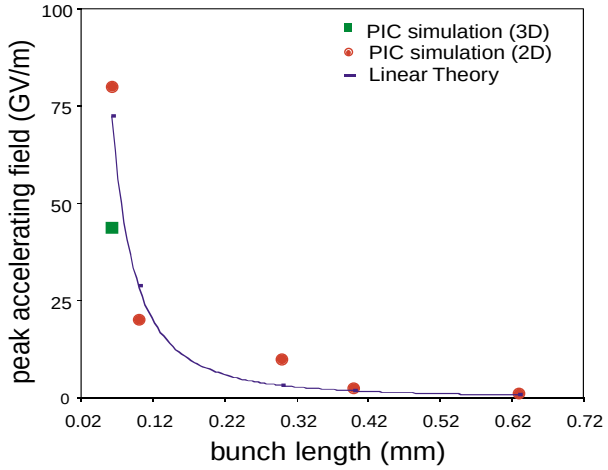

FIG. 2. (Color) Particle-in-cell simulation results for the peak plasma wake amplitude versus bunch length. The solid curve shows the scaling from linear theory [Eq. (1)]. In these simulations, the cell size was kept at $0.1c/\omega_p$ in the transverse direction, $0.05c/\omega_p$ longitudinally, nine particles/cell (4 in 3D), and the plasma density was adjusted to maintain $k_p\sigma_z \cong \sqrt{2}$. The width of the system was adjusted to ensure that the plasma blowout did not reach the walls (typically $6c/\omega_p$).

where σ_z is the Gaussian bunch length and $k_p = \omega_p/c$ is 1 over the plasma skin depth ($c/\sqrt{4\pi n_o e^2/m}$). In this case, the wake amplitude scales linearly in the bunch charge and inversely with the square of the bunch length:

$$eE_o \approx 240\ (\mathrm{MeV/m})\left(\frac{N}{4\times 10^{10}}\right)\left(\frac{0.6\ \mathrm{mm}}{\sigma_z}\right)^2. \quad (1)$$

This strong bunch length dependence is a primary motivator for this work. It suggests that simply decreasing the bunch length by a factor of 10 from present SLAC parameters could increase the wake field amplitude by 100. However, this is strictly valid only within the limits of linear theory, i.e., $n_b \ll n_o$. For the parameters typical of the SLC bunches and the plasmas of interest for high gradient acceleration, this inequality is not fulfilled. Thus, we turn instead to numerical simulations.

To study the wake field excitation scaling laws in the nonlinear regime of $n_b > n_o$, we employ the 3D fully self-consistent and object-oriented model OSIRIS. The simulation model has been described in more detail elsewhere [9,10]. It follows 10^6–10^8 particles on a 2D or 3D moving mesh of 10^5–10^6 cells. The beam and plasma particles move according to the Lorentz force and their self-consistent electromagnetic fields, found by solving Maxwell's equations on the grid. This code and others have been used previously to model nonlinear wake fields excited by electron bunches with densities a few times the plasma density [1]. Here we extend that work by considering much shorter bunches for which the beam density far exceeds the plasma density.

Figure 2 shows the results of several simulation runs to measure peak wake amplitude versus bunch length. For each case, the number of particles is kept fixed ($N = 4\times 10^{10}$) and the plasma density is adjusted to match to the bunch length. The solid curve is the linear theory prediction. Although the wakes are highly nonlinear, the linear theory expression for the amplitude is in good agreement with the simulations up to values of $E/E_D \sim 5$, where E_D is the Dawson nonrelativistic wave breaking field ($\sim\sqrt{n_o}$ V/cm) [11]. We comment that the optimal plasma density for a given bunch length is slightly higher than the linear theory expression above. This is because of the nonlinear frequency shift of the plasma wave at large amplitude. This shift toward lower frequency arises from the relativistic mass increase of the oscillating plasma electrons.

A sample snapshot of the plasma wake fields excited by a short electron bunch is shown in Fig. 3a. In this example, the electron bunch consisted of a 3×10^{10} electron in a bi-Gaussian distribution of radius $\sigma_r = 25\ \mu$m and length $\sigma_z = 63\ \mu$m (10 times shorter than is typical of the current SLC beam). The plasma density was chosen to be 1.8×10^{16} cm^{-3} corresponding approximately to the plasma matching discussed above. The peak beam density

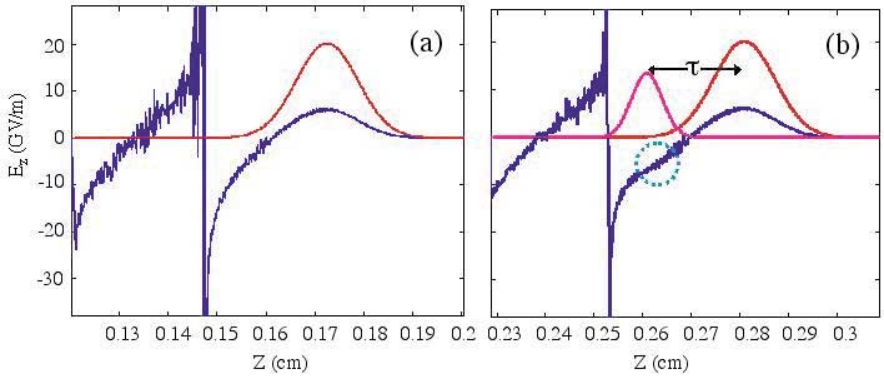

FIG. 3. (Color) Longitudinal plasma wake fields on the axis for the beam profiles shown. (a) Drive bunch only and (b) drive bunch and trailing bunch separated by delay τ. Note flattening of wake due to beam loading shown in the dotted area.

is 4.8×10^{16} cm^{-3}, well above the plasma density. Accordingly, the plasma response is very nonlinear as seen in Fig. 3. A large spike in the longitudinal field is apparent where the plasma electrons that were expelled by the beam have returned to the axis. The peak accelerating field (i.e., amplitude of the spike) is 80 GeV/m for this case. The focusing force is nearly constant ahead of the spike at the value $2\pi n_o e^2 r$, as one would obtain from the bare space charge of a positive ion column.

The results in Figs. 2 and 3 are suggestive. With fields of several tens of GeV/m, it would appear to be possible to double the energy of a 50 GeV collider with plasma afterburner sections that are only a few meters long. The realization of this promise is contingent upon a number of physics and technology issues. These are described next. They include (i) beam loading (generating and phasing very short bunches), (ii) transverse beam dynamics (betatron oscillations and emittance growth as well as electron hose instability), (iii) plasma source development, (iv) positron acceleration, and (v) modeling.

Beam loading and phasing.—We consider a two bunch system consisting of a driver bunch and a trailer bunch separated by a small distance such that the trailer sits near the peak wake field of the driver. One possible means to achieve a double-bunch arrangement in the SLC is to use a bunch compression system operating in a mode so as to overbunch a single bunch. To obtain a modest energy spread of the accelerated bunch requires that the second bunch not only be properly phased but also shorter than the first. To be specific, we take the following parameters for a round beam example. Drive beam number and size: $N = 3 \times 10^{10}$, $\sigma_z = 63$ μm, $\sigma_r = 25$ μm; trailer beam: $N = 1 \times 10^{10}$, $\sigma_z = 32$ μm, $\sigma_r = 25$ μm; plasma density and length: $n_o = 1.8 \times 10^{16}$ cm^{-3}, $L \sim 7$ m.

The spacing between the microbunches is determined empirically from simulations. Figure 3b shows a snapshot of the wake due to the two bunches. By comparing to the unloaded wake in Fig. 3a, we see the absorption of the wake due to the nonlinear beam loading by the second bunch. We performed several simulation runs with different phasing of the load. Increasing the phase delay increases the peak energy and the energy spread. The delay for this case was 0.6 ps giving an average energy gain rate of 8 GeV/m with a FWHM spread of 20%. We note that the maximum decelerating field on the driving bunch is 7 GeV/m. Thus neglecting deformation of the bunches, they could propagate a distance of 7 m, imparting an energy of 56 GeV to the trailing bunch.

We note that this beam loading example is not optimized. For example, slightly more charge in the bunch load could further flatten the wake at the beam load (see Fig. 3b) and reduce the energy spread. Moreover, it is possible to more than double the energy of the trailing bunch by increasing the phase delay of the bunch load so as to sample the larger electric field near the spike. However, the steepening of the wave form near the spike requires the beam load to be even shorter and narrower. Naturally, fewer particles can be supported by the field energy there (as is also apparent from energy conservation), so one must choose how much to trade off luminosity for higher energy.

Transverse beam dynamics.—A great deal of information about transverse beam propagation issues has been learned from a recent meter-long plasma wake field experiment at SLAC known as E-157 [3]. Of primary concern are betatron oscillations and hose instabilities. While there were nominally three to five betatron oscillations in E-157, there will be roughly 100 over the length of an afterburner. If there is phase mixing due to longitudinal and transverse focusing aberrations, there will be an unrecoverable emittance growth. To prevent this, the beta functions of the beam and the plasma focusing must be matched [4]. The matching condition for electrons is

$$\gamma \varepsilon^2 / \sigma^4 = 2\pi n_o r_e \,, \tag{2}$$

where ε is the beam emittance, γ is its energy, σ its spot size, and r_e is the classical electron radius. This will require beams to be of the order of 1 μm in radius at the plasma entrance (1.3 μm for a normalized emittance of 10 mm mrad at 50 GeV) or an adiabatic plasma transition section. The modeling of submicron beams with particle-in-cell simulations requires a resolution that challenges the capability of current computers.

A second transverse issue is the electron hose instability. Simple analytic estimates [12,13] suggest that there may be of the order of 10 e-foldings of hose growth for afterburner parameters. However, the electron hose instability was not observed experimentally in E-157 even though up to three e-foldings were predicted. The experiment was in agreement with simulations that showed that E-157 is near the margin for hose instability. Further work is needed to study hosing for afterburner parameters and to address stabilization mechanisms such as transverse plasma gradients.

A third transverse issue arises from the plasma lenses at the end of the acceleration sections. It is straightforward to estimate from the envelope equation for an electron beam [14] the spot size reduction possible by a plasma lens [15]. For a plasma lens of density n_l satisfying $n_b \gg n_l \gg n_o$, and assuming that the normalized emittance is preserved in the plasma, the spot size can be compressed by a factor of $\sqrt{n_l/n_o}$. For the example above, a short (approximately 2 mm) plasma section of density 2×10^{18} cm^{-3} would reduce the spot size from the order of 1 μm to the order of 100 nm.

Plasma source development.—The plasma parameters in the afterburner example above somewhat exceed the state of the art in terms of the production of long high-density plasmas. Just how the plasma density can be stepped up for the plasma lenses and how the walls of the plasma device can be made compatible with the detector

design are also unresolved issues. An important research direction then is the development of new plasma production techniques. Beam ionization of gas and resonant laser ionization are promising possibilities requiring experimental investigation [16].

Positron acceleration.—In the nonlinear regime here, the wake excitation by positron beams is not symmetric to the electron case. In recent work [17], simulations showed that positron wakes are typically smaller than electron wakes due to phase mixing of the arrival time of plasma electrons sucked into the beam axis. However, the positron wakes can become comparable to the electron wakes if a hollow or ring-shaped plasma of radius c/ω_p is used. Just such a profile was demonstrated by blocking the center of the ionizing laser at the E-157 laboratory. Experimental investigation of nonlinear positron wakes and positron propagation and acceleration is of great importance for further assessment of this scheme.

The work presented here suggests a promising path for achieving a breakthrough in advanced accelerator development. Preliminary simulations support the possibility of an energy doubler for linear colliders based on short plasma wake field sections placed just before the collision point. A concerted research effort to demonstrate control of transverse instabilities, develop plasma sources of sufficient length and density, and produce short microbunches is the key to realizing this concept.

ACKNOWLEDGMENTS

This work was supported by U.S. Department of Energy Contracts No. DE-FG03-92ER40745, No. DE-FG03-98DP00211, No. DE-FG03-92ER40727, and No. DE-AC03-765F00515, NSF Contracts No. ECS-9632735 and No. DMS-9722121, and LLNL Contract No. W07405-ENG48. We are indebted to the late John Dawson for his early vision of boosting the energy of linear colliders with plasma wake field sections, and we acknowledge stimulating conversations with David Sutter at the 1999 Particle Accelerator Conference and Marty Breidenbach at SLAC that prompted us to undertake this design study. Ongoing discussions with Robert Siemann are gratefully acknowledged.

[1] O. Morton, Science **289**, 2014 (2000).
[2] O. Morton, Science **290**, 1274 (2000).
[3] M. J. Hogan *et al.,* Phys. Plasmas **7**, 224 (2000).
[4] P. Muggli *et al.,* Nature (London) **411**, 43 (2001).
[5] S. Lee, T. Katsouleas, R. Hemker, and W. B. Mori, Phys. Rev. E **61**, 7014 (2000).
[6] R. G. Hemker, W. B. Mori, S. Lee, and T. Katsouleas, Phys. Rev. ST Accel. Beams **3**, 061301 (2000).
[7] N. Barov, J. B. Rosenzweig, M. E. Conde, W. Gai, and J. G. Power, Phys. Rev. ST Accel. Beams **3**, 011301 (2000).
[8] R. Keinigs and M. E. Jones, Phys. Fluids **30**, 252 (1987).
[9] R. G. Hemker, F. S. Tsung, V. K. Decyk, W. B. Mori, S. Lee, and T. Katsouleas, in *Proceedings of the 1999 Particle Accelerator Conference, New York* (IEEE, Piscataway, NJ, 1999), p. 3672.
[10] R. Hemker, Ph.D thesis, University of California, Los Angeles, 2000.
[11] J. M. Dawson, Phys. Rev. **133**, 383 (1959).
[12] A. Geraci and D. Whittum, Phys. Plasmas **7**, 3431 (2000).
[13] E. Dodd *et al.,* Phys. Rev. Lett. (to be published).
[14] C. Clayton *et al.,* Phys. Rev. Lett. (to be published).
[15] P. Chen, Part. Accel. **20**, 171 (1985).
[16] C. Joshi (private communication).
[17] S. Lee *et al.,* Phys. Rev. E **64**, 045501 (2001).

REVIEW PAPERS

High energy density plasma science with an ultrarelativistic electron beam[a)]

C. Joshi,[b)] B. Blue, C. E. Clayton, E. Dodd, C. Huang, K. A. Marsh, W. B. Mori, and S. Wang
University of California Los Angeles, Los Angeles, California 90095

M. J. Hogan, C. O'Connell, R. Siemann, and D. Watz
Stanford Linear Accelerator Center, Stanford University, Stanford, California 94309

P. Muggli, T. Katsouleas, and S. Lee
University of Southern California, Los Angeles, California 90089

(Received 2 November 2001; accepted 3 January 2002)

An intense, high-energy electron or positron beam can have focused intensities rivaling those of today's most powerful laser beams. For example, the 5 ps (full-width, half-maximum), 50 GeV beam at the Stanford Linear Accelerator Center (SLAC) at 1 kA and focused to a 3 micron rms spot size gives intensities of $>10^{20}$ W/cm^{-2} at a repetition rate of >10 Hz. Unlike a ps or fs laser pulse which interacts with the surface of a solid target, the particle beam can readily tunnel through tens of cm of steel. However, the same particle beam can be manipulated quite effectively by a plasma that is a million times less dense than air! This is because of the incredibly strong collective fields induced in the plasma by the Coulomb force of the beam. The collective fields in turn react back onto the beam leading to many clearly observable phenomena. The beam paraticles can be: (1) Deflected leading to focusing, defocusing, or even steering of the beam; (2) undulated causing the emission of spontaneous betatron x-ray radiation and; (3) accelerated or decelerated by the plasma fields. Using the 28.5 GeV electron beam from the SLAC linac a series of experiments have been carried out that demonstrate clearly many of the above mentioned effects. The results can be compared with theoretical predictions and with two-dimensional and three-dimensional, one-to-one, particle-in-cell code simulations. These phenomena may have practical applications in future technologies including optical elements in particle beam lines, synchrotron light sources, and ultrahigh gradient accelerators. [DOI: 10.1063/1.1455003]

I. INTRODUCTION

Historically, high energy density plasma science (HEDPS)[1] refers to the study of high-temperature, high-density plasmas produced by a number of different types of drivers: Lasers, ion beams, *z*-pinches and modestly relativistic ($\gamma<10$) electron beams. HEDPS with an ultrarelativistic electron beam, U-REB, ($\gamma\gg10^3$) has hitherto not been explored despite the fact that the energy density associated with such a driver can be comparable to that of the most powerful other types of drivers mentioned above that are used in HEDPS. Table I below compares, for instance, the driver parameters of a 100 TW, 30 fs laser, and the existing nominally 50 GeV electron beam at the Stanford Linear Accelerator Center (SLAC).

As can be seen from Table I, the peak intensities achieved at the focus of these two drivers for HEDPS are comparable. However, the interaction of photons and electrons as they impact a solid target is very different. Unlike a fs laser pulse, which even at these ultrahigh intensities is strongly attenuated by a thin layer of plasma formed by the photons at the target surface, the U-REB can readily tunnel through tens of cm of steel. On the other hand the interaction of both an intense laser pulse and a high current electron pulse with the plasma can be qualitatively very similar when the two propagate through a low-density plasma. In either case a significant amount of drive beam energy can be transferred to the plasma electrons making them relativistic particularly in the electron blow-out regime.[2] In the laser beam case each electron receives energy on the order $(v_0/c)^2mc^2$ whereas in the electron beam case each electron receives $\sim(n_b/n_p)^{1/2}mc^2$ amount of energy. The symbols are defined in Table II. In this sense this is a distinctly different regime of HEDPS that has not been systematically explored until now. The main motivation for using U-REBs in the plasmas is the development of the beam-driven plasma wakefield accelerator. The focus of this research is on demonstrating accelerating gradients on the order of 1 GeV/m over a meter of

[a)]Paper JR1 1, Bull. Am. Phys. Soc. **46**, 172 (2001).
[b)]Invited speaker.

TABLE I. Physical characteristics of a state-of-the-art laser and particle beams.

	100 TW laser	50 GeV electron beam
Energy per particle (eV)	1.5	50×10^{9}
Pulse length (FWHM) (ps)	30×10^{-3}	5
Spot size (μm)	5	3
Energy/pulse (J)	3	150
Rep rate (Hz)	100	10–120
Peak intensity (W/cm^2)	10^{20}	10^{20}

plasma. Such large fields can only be excited over this length using an U-REB.

The physical mechanisms are quite different in the laser and the beam cases but the experimentally observable effects are similar. For instance, the laser pulse interacts with the plasma electrons via the ponderomotive force which is proportional to the gradient of the intensity, whereas the U-REB plasma interaction is via the space charge electric field of the electron beam. In the so-called ''blow-out'' regime[2] (which for laser pulses occurs when $v_0/c \gg 1$ and $k_p\sigma_r \ll 1$ and for an electron pulse occurs when $n_b \gg n_p$ and $k_p\sigma_r \ll 1$) both drivers expel all the plasma electrons [on a time scale of either ω_p^{-1} laser or ω_b^{-1} (beam)] and create an ion channel. The effect of the ion channel on the photons is relatively weak arising from the modified index of refraction of the plasma. However, that is not the case for a U-REB. The space-charge force of the ion channel can influence the electron bunch in profound ways depending on certain initial conditions. In a general sense one can observe all the same effects as one would when a charged particle interacts with an electric field: Deflection, acceleration, and radiation. In the case of an electron beam these effects can be observed as (a) focusing of the beam outside the plasma, (b) deflection or steering of the beam, (c) periodic oscillations of the beam spot, (d) emission of wiggler radiation in the x-ray range, (e) deceleration of the bulk of the beam, and (f) acceleration of some beam particles in the tail of the beam. Some of these effects have been studied using lower energy relativisic electron beams propagating through plasmas,[3–6] but a systematic study of all these effects under the same experimental conditions has never been carried out to date using an U-REB. There is hope that phenomena being studied here will lead to the development of new plasma technologies including new types of lenses and kickers for future high-energy particle beam lines, plasma wigglers and undulators for the next generation of synchrotron light sources, an entirely new paradigm for building high-gradient accelerators and a new class of free electron lasers.

TABLE II. Definition of parameters used in text. All other symbols are as defined in the NRL Plasma Formulary (Ref. 10).

Physical parameter	Symbol/formula
Total number of beam particles	N
Initial position of the electron	r_0
Longitudinal r.m.s. size of beam	σ_z
Transverse r.m.s. size of the beam	$\sigma_x, \sigma_y, \sigma_r$
Beam (plasma) density	$n_b(n_p)$
Laser frequency (field)	ω, E_L
Normalized electron velocity	$\beta = v/c$
Longitudinal electric field	eE
Lorentz factor of the beam	$\gamma = (1-\beta^2)^{-1/2}$
Electron beam density	$n_{b0} = N/(2\pi)^{3/2}\sigma_r^2\sigma_z$
Electron plasma frequency	$\omega_p = (n_p e^2/\varepsilon_0 m)^{1/2}$
Beam plasma frequency	$\omega_b = (n_{b0} e^2/\varepsilon_0 m)^{1/2}$
Collisionless skin-depth	c/ω_p
Plasma wave number	$k_p = \omega_p/c = 2\pi/\lambda_p$
Normalized emittance of the beam	$\varepsilon_N = \gamma\varepsilon$
Focusing beta of the beam	$\beta_{\text{beam}} = \gamma\sigma_r^2/\varepsilon_N$
Effective wiggler strength	$a = \gamma k_\beta r_o$
Betatron frequency	$\omega_\beta = \omega_p/(2\gamma)^{1/2}$
Betatron wave number	$k_\beta = \omega_\beta/c$
Matched beam radius	$r_{bm} = (\varepsilon_N/\gamma k_p)^{1/2}$
Wake amplitude	$n_1/n = eE/m\omega_p c$
Electron oscillatory velocity	$v_0/c = eE_L/m\omega c$

TABLE III. Typical beam and plasma parameters used in the experiments.

Number of e^- per bunch	N	$1.8–2\times10^{10}$
Bunch energy	E, γ	28.5 GeV, 5.58×10^3
Bunch radius	$\sigma_r, \sigma_x, \sigma_y$	30–40 μm
Bunch length	σ_z	0.7 mm
Beam density	n_b	1.5×10^{15} cm^{-3}
Normalized emittance	$\varepsilon_{N,x}$	5×10^{-5} m-rad
Plasma density	$\varepsilon_{N,y}$	0.5×10^{-5} m-rad
Plasma length	L	1.4 m

II. EXPERIMENTAL CONDITIONS

The experimental work discussed in this review paper was carried at SLAC as part of two experimental investigations, E157 and E162, using the U-REB at the Final Focus Test Beam (FFTB) facility. The beam parameters are shown in Table III. These do not include the effect of foils and pellicles used in the experiment.[7] Unless explicitly mentioned otherwise, these parameters were used in the various experiments.

The experimental set-up has been described in detail in Ref. 7. We will describe the apparatus briefly in this article so that the experimental data presented later can be understood easily.

Figure 1 shows the schematic of the experimental set-up. The SLAC beam with the above mentioned parameters was focused near the entrance of a lithium plasma produced by photo-ionization of a 1.4 meter long lithium vapor column by an ArF laser.[8] The beam size (σ_x, σ_y), 1 m upstream and 1 m downstream of the plasma was recorded by imaging the optical transition radiation (OTR),[9] produced by the beam, onto 16 bit charge coupled device (CCD) cameras. The electron beam exiting the plasma was bent or dispersed in the vertical or *y*-plane using a 5.2 m long dipole bending magnet placed 3 m from the plasma exit.

The dipole magnet provided a net dispersion of 300 MeV/mm at a 1 mm thick aerogel Cherenkov radiator placed 12 m from the plasma. The Cherenkov light was split using a beam-splitter and sent to a 16 bit CCD camera to record the time integrated beam profile or to a streak camera where it was time resolved in both planes, (x vs τ) and (y vs τ), with an $\sim$2 ps resolution, here τ is the time measured from the center of the bunch. The forward emitted x-ray radiation

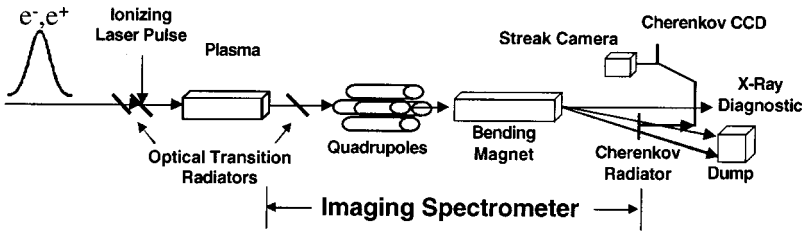

FIG. 1. The experimental set-up for studying beam-plasma interaction effects with a 28.5 GeV electron or positron beam that was used in most of the experiments described in the text. The detection set-up for x-rays in the forward direction is not shown.

from the plasma was reflected using a Si(111) crystal and recorded using two surface barrier detectors. The electron beam position downstream of the plasma was measured by a series of stripline beam position monitors (BPMs).

III. HIGH ENERGY DENSITY PLASMA SCIENCE (HEDPS) IN BEAM–PLASMA INTERACTION

The electron beam has a Gaussian profile in both transverse and longitudinal directions given by

$$n_b(x,y,z)=n_{b0}e^{-x^2/2\sigma_x^2}e^{-y^2/2\sigma_y^2}e^{-z^2/2\sigma_z^2}, \tag{1}$$

where for a round beam the total number of beam particles is given by

$$N=\int_{z=-\infty}^{\infty}\int_{r=0}^{\infty}n_b(x,y,z)2\pi r dr dz, \tag{2}$$

from which we obtain the peak beam density as

$$n_{b0}=\frac{N}{(2\pi)^{3/2}\sigma_r^2\sigma_z}. \tag{3}$$

It is well-known that for a relativistic beam the radial space charge force and the self-magnetic force counter and cancel each other to the order $1/\gamma^2$.[11] Thus an initially collimated U-REB propagates in vacuum with an expanding envelope due mainly to its intrinsic emittance.

When such a beam is injected into a plasma, the plasma electrons begin to be expelled from a region surrounding the beam in order to preserve the charge neutrality of the plasma. This in turn perturbs the belance between the self-forces of the beam mentioned above. What then happens to the beam depends on the relative beam and plasma parameters. If $n_p > n_b$ and $k_p\sigma_r \ll 1$, the beam is self-pinched by its own magnetic field.[12] On the other hand if $n_b > n_p$, known as the underdense plasma condition, the beam electrons blow out the plasma electrons leaving behind an ion column.[13] The ion column in turn exerts a focusing force on the beam. It is this latter regime of propagation, known as the ion focused regime that is of interest to this work.

The formation of the ion channel and the action of the ion channel back on the beam are both transient effects for beams that are both narrow, $k_p\sigma_r \ll 1$, and short $k_p\sigma_z \sim 0(1)$. Nevertheless, the radius of the ion channel that is formed can be estimated by equating the space-charge field of the beam and the electrostatic field of the ion column at this radius[14] leading to

$$r_i=\sigma_r\left(\frac{n_{b0}}{n_p}\right)^{1/2}. \tag{4}$$

For $n_{b0} \gg n_p$, plasma electrons are blown out from a region of plasma that is much wider than the beam spot size.

There are now a number of physical effects that ensue as the ion channel exerts a focusing force on the electron beam. The radial electrostatic field of this ion[15] channel is given by

$$E_r=\frac{1}{2}\frac{n_p e}{\varepsilon_0}r, \tag{5}$$

which varies linearly with r. Substituting $r=\sigma_r$ leads to

$$E_r=9\times10^{-15}n_p\,[\mathrm{cm}^{-3}]\,\sigma_r\,[\mu\mathrm{m}]\,\mathrm{MV/m}. \tag{6}$$

This radial electric field has profound transverse and longitudinal effects on the beam which we will discuss. Of particular interest is the case when $k_p\sigma_z \sim 0(1)$, for which a strong longitudinal electric field is excited behind the head of the beam.

A. Beam focusing or underdense plasma lensing

It can be seen from Eq. (5) that in the underdense regime, the ion column exerts a focusing force that increases with r and, therefore, a section of plasma acting as a focusing lens has, in principle, no spherical aberrations. However such a lens still has longitudinal and chromatic aberrations. Spherical aberrations are caused by the time dependence of ion channel formation whereas the chromatic aberrations arise from the energy variations within the beam. The effective focusing gradient can be found from Eq. (1) as

$$B_\theta/r=3\times10^{-9}n_p\,[\mathrm{cm}^{-3}]\,\mathrm{G/cm}. \tag{7}$$

In the thin lens approximation the electron beam after traversing a length L of an ion column with density n_p will focus at[16]

$$f=\frac{2\gamma c^2}{L\omega_p^2}=5.6\times10^{11}\frac{\gamma}{L(\mathrm{cm})n_p(\mathrm{cm}^{-3})}. \tag{8}$$

As an example, using Eqs. (7) and (8) a 10 cm long, 10^{15} cm^{-3} density plasma lens will have a focusing gradient of 3 MG/cm and will focus a 50 GeV SLAC beam in just 8.6 cm.

Consider the case of a beam of emittance ε focused to a spot size σ_0^* at a distance s_0 away. The initial beam β is related to the beam beta at the waist ($\beta_0^*=\sigma_0^*/c$) by

$$\beta=\beta_0^*\left(1+\frac{s_0^2}{\beta_0^{*2}}\right). \tag{9}$$

When the beam traverses a thick lens of length L ($L \ll s_0$) and density n_p, the beam beta at the lens exit is given by

TABLE IV. Plasma lens characteristics for three incident spot sizes.

Initial spot size σ_o^* (μm)	Final spot size n_b/n_p	σ_x^* (μm)	σ_y^* (μm)	Focal length f_x (μm)	f_y (μm)	$(c/\omega_{pb})/\sigma_z$
50	4	6	1.5	24.4	24.7	0.24
40	6.5	7.4	1.9	23.8	24.7	0.19
30	11	9.6	2.5	22.2	24.6	0.14

$$\beta_L=\frac{\beta_0}{2}+\frac{1}{2K\beta_0^*}+\left(\frac{\beta_0}{2}-\frac{1}{2K\beta_0^*}\right)\cos(2\sqrt{K}L)$$
$$-\frac{2s_0}{2\sqrt{K}\beta_0^*}\sin(2\sqrt{K}L), \tag{10}$$

where $K=\omega_p^2/2\gamma c^2$. The beam beta at the new waist is given by[17]

$$\beta^*=\frac{\beta_0^*}{1+K(\beta_0-\beta^*)\beta_0^*} \tag{11}$$

and the new waist is located at a distance s from the lens entrance given by

$$s=(\beta^*(\beta_L-\beta^*))^{1/2}. \tag{12}$$

The demagnification ratio defined as $\sigma_0^*/\sigma^*=(\beta_0^*/\beta^*)^{1/2}$ can be maximized with respect to σ_0^*, n_p, and L. Table IV illustrates the effect of varying the initial spot size σ_0^* on the final spot size σ^*. Plasma parameters were: $n_p=1.2\times10^{14}$ cm^{-3}, $L=10$ cm. The beam parameters were: $N=2\times10^{10}$ electrons, $\sigma_z=1$ mm, $\varepsilon_{Nx}=60$ mm-mrad, and $\varepsilon_{Ny}=15$ mm-mrad. As σ_0^* is decreased, the n_b/n_p ratio increases causing the blow-out to be reached earlier in the bunch. The longitudinal aberrations are thereby reduced. However, as σ_0^* is decreased the minimum spot size increases because of the beam emittance contribution to σ^* in these examples. Note that the focal length of the lens is relatively independent of σ_0^*, and that the values of σ^* are different in the x and y planes because $\varepsilon_{Nx}\neq\varepsilon_{Ny}$.

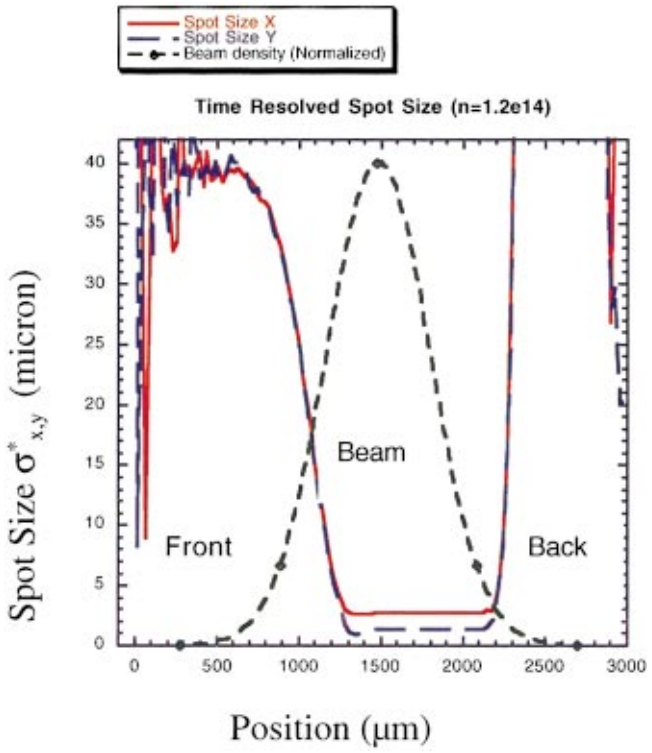

FIG. 2. (Color) Simulation results from code QUICKPIC showing time dependent focusing for a 28.5 GeV beam after traversing a 10 cm long, 1.2×10^{14} cm^{-3} plasma at 25 cm from the plasma exit in both x and y transverse directions. The beam waist is placed at the plasma entrance.

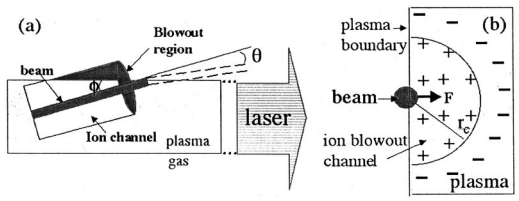

FIG. 3. Physical mechanism for collective "refraction" of a relativistic electron beam traversing a plasma/neutral gas boundary: (a) Side view and (b) front view of beam and plasma illustrating how asymmetric blowout creates a net deflection force F.

The predictions of the analytical theory have been tested using the 3D quasi-state, particle-in-cell (PIC) code QUICKPIC.[18] The initial beam and plasma parameters are those of the $\sigma_0^*=50$ μm case in Table IV. Figure 2 shows that the spot sizes at the beam waist located 25 cm downstream of the lens exit are $\sigma_x^*=5$ μm and $\sigma_y^*=2$ μm, respectively. These values are in excellent agreement with those obtained from the analytical model (Table IV). The choice of n_p and σ_z in this example is such that $k_p\sigma_z\cong\sqrt{2}$, therefore, the plasma electrons thus rush back on axis in the back of the electron bunch. They create a defocusing force that causes $\sigma_{x,y}^*$ to blow up in the back of the bunch (position >2300 μm on Fig. 2).

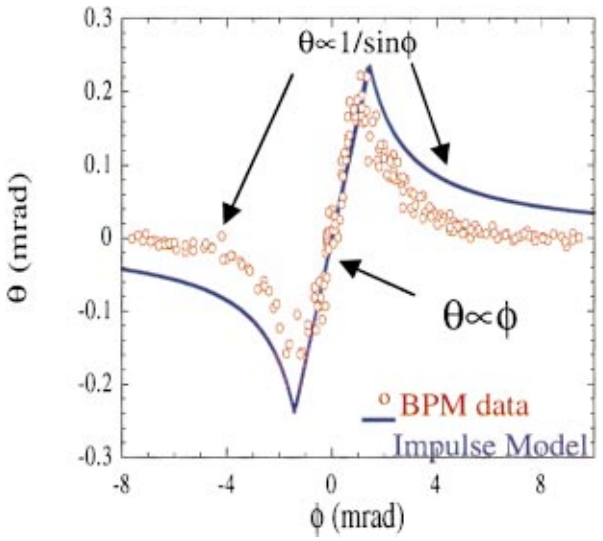

FIG. 4. (Color) A plot of beam deflection angle θ measured with a beam position monitor versus angle between the ionizing laser and the beam ϕ. ϕ is also the angle between the beam and the plasma. For incident angles ϕ less than 1.2 mrad the beam appears to be internally reflected. The solid line is the prediction of the simple impulse model described in the text.

In the above examples the demagnification factors are between 10 and 25. Plasma lenses with large demagnification factors will be highly desirable for increasing the luminosity in future linear colliders. However, the penalty for doing so may be a significant synchrotron energy loss resulting in background problems at the detector.

B. Collective refraction of the beam

If the electron beam is propagated at an angle ϕ with respect to the axis of the plasma column such that it encounters a plasma–vacuum or a plasma–neutral gas boundary, it can experience a deflection which can be thought of as a collective refraction effect. Under certain conditions the beam is not only refracted away from the normal it can actually be totally internally reflected as a photon beam would do in an optical fiber. As discussed above, when the beam is fully inside the plasma, the head of the beam expels the plasma electrons out to a radius r_i. As the beam approaches the plasma-gas boundary the ion channel becomes asymmetric as shown in Figs. 3(a) and 3(b). This causes the beam to be deflected towards the plasma.

The magnitude of this deflection has been estimated using an impulse model.[19] As the beam approaches the plasma–neutral gas boundary at an angle ϕ, the force on the beam due to the ion channel of radius r_i is given by Gauss's law as

$$F=-2n_p e^2 r_i .$$

The beam spends roughly $2r_i/c \sin\phi$ amount of time near the edge. The impulse on the beam is thus the Coulomb force multiplied by the time that the beam resides within the ion channel. Dividing by the beam's parallel momentum γmc gives a scaling law for the deflection angle θ, valid for $\phi > \theta$ as

$$\theta=\frac{8}{\pi}\frac{\alpha N r_e}{\sqrt{2\pi}\gamma\sigma_z \sin\phi}, \tag{13}$$

where $eN/\sqrt{2\pi}\sigma_z$ is the charge per unit length of the beam and α is a numerical factor which is <2 for beams that are longer than λ_p.

The impulse model breaks down at small angles of incidence ϕ such that the deflection angle θ is on the order of ϕ. In this case the beam can be totally internally reflected. This is a collective refraction effect whose magnitude in a rather dilute plasma of density $\sim 10^{14}$ cm^{-3} (typically $\phi<1$ mrad as will be seen later) can be orders of magnitude greater than that expected from single electron considerations.

We have experimentally demonstrated this ''refraction'' effect by deliberately propagating the electron beam at an angle ϕ with respect to the plama column. Figure 4(a) shows the actual electron–beam deflection (circles) measured using a BPM and the theoretical deflection (solid line) as a function of ϕ. $\phi=0$ degrees means that the U-REB and the ionizing laser are exactly co-propagating. By varying the angle the laser makes with respect to the electrons, the electron beam can be made to exit from either side of the plasma column. When the angle of deflection θ is plotted against the incident angle ϕ, this gives to a symmetric curve about $\theta=0$ degrees. For incident angles up to 1.2 mrad the deflection is seen to be proportional to $1/\sin\phi$ as predicted. However, for $\phi<1.2$ mrad the beam appears to be totally internally reflected, i.e., $\theta\propto\phi$, again in good agreement with the theoretical model. It is remarkable that a 28.5 GeV beam that is able to tunnel through several centimeters of steel is totally internally reflected, by collective fields of plasma that is roughly million times less dense than air.

C. Betatron oscillations of the beam envelope

If the density length product of the plasma is large enough, the electron beam can focus within the plasma itself. As the plasma density is further increased the electron beam can undergo multiple betatron oscillations inside the plasma.[20] The behavior of the electron beam with a normalized emittance ε_N is described by the beam envelope equation

$$\sigma_r''(z)+\left[K^2-\frac{\varepsilon_N^2}{\gamma^2\sigma_r^4(z)}\right]\sigma_r(z)=0, \tag{14}$$

where $K=\omega_p/(2\gamma)^{1/2}c$ is the restoring constant of the plasma or equivalently the betatron wave number k_β. The beam is said to be matched to the plasma if $\beta_{\text{beam}}=1/K=\beta_{\text{plasma}}$. In this case the beam radius remains constant as the beam propagates through the plasma. This matched beam radius r_{bm} is found by letting $\sigma''(z)=0$ in Eq. (12) giving $r_{bm}=(\varepsilon_N/\gamma k_p)^{1/2}$. If the initial beam radius is larger than r_{bm} then the beam *envelope* oscillates with a spatial period π/K which is equal to half the individual particles' betatron wavelength. The beam particles exit the plasma with a well defined deflection angle

$$\sigma_r'=\sigma_r k_\beta|\sin k_\beta z|. \tag{15}$$

The phase advance experienced by the beam envelope in a plasma of density n_p and length L is

$$\Psi_L(n_p)=\int_0^L K dz=K(n_p)L\ \alpha\ n_p^{1/2}. \tag{16}$$

It is clear that whenever $\Psi_L(n_p)=m\pi$ radian the beam size at the exit of the plasma will be the same as the beam size at the entrance of the plasma. At these values of phase advance the exit angle is zero for a beam that is focused to a waist at the plasma entrance, and therefore, the beam is transparent to the plasma. On the other hand, whenever $\Psi_L(n_p)=(m+1)\pi/2$ radian the beam exits the plasma at a focus and with a maximum divergence angle which scales as k_β or $\sqrt{n_p}$.

The above discussion is strictly valid for the steady state propagation of a beam in a preformed ion channel. If the ion channel is induced by the beam itself which has a finite rise-time, different longitudinal slices of the beam can undergo different number of betatron oscillations in a plasma with a given product n_pL. However, if $n_{b0}>n_p$ most of the beam can be affected by the ion channel that is fully denuded of plasma electrons. Thus, the envelope equation can be used to compare experiments with theory. In the experiment the beam spot size cannot be measured inside the plasma. It is usually measured at some distance outside of the plasma as

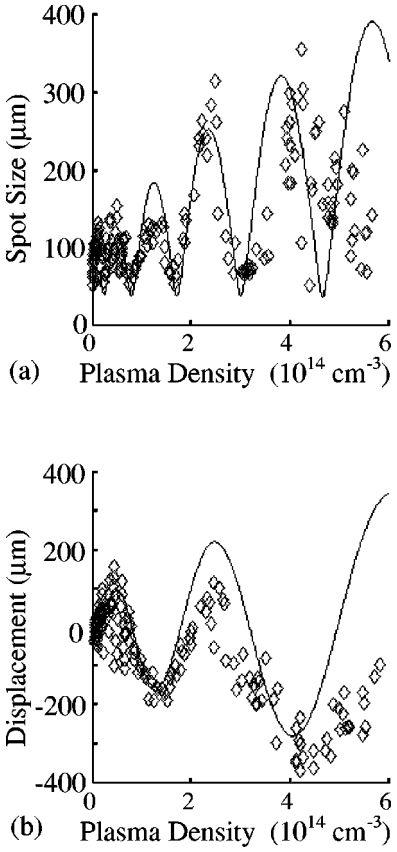

FIG. 5. (a) Multiple oscillations of the spot-size due to betatron motion of a 28.5 GeV electron beam in a 1.4 m long lithium plasma as the plasma density is increased. The solid line is a theory fit to the measured data using the beam envelope equation, Eq. (14). (b) Centroid oscillations of a 28.5 GeV electron beam measured using the downstream OTR detector as a function of plasma density. Solid line is the prediction of the envelope equation, Eq. (14) with $\varepsilon_N = 0$.

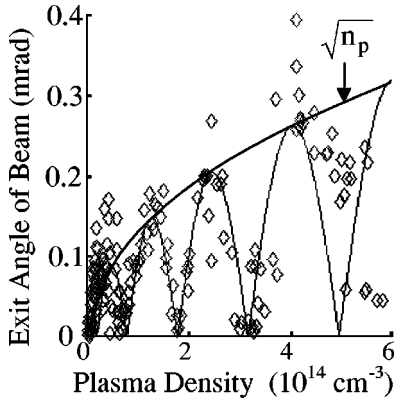

FIG. 6. Exit angle of a 28.5 GeV beam after traversing a 1.4 m long plasma whose density is being increased. The solid curve is the prediction of the theory, Eq. (15). The peaks angles increase as k_β or $\sqrt{n_p}$ as shown by the solid parabola.

the plasma density, and therefore, Ψ_L is varied. The measured spot size can thus be compared as a function of Ψ_L using Eq. (14).

In recent experiments (with beam parameters given in Table III) multiple, betatron oscillations of the beam inside the plasma are clearly inferred from oscillations of the spot size of the beam as observed 1 m downstream of the plasma by imaging the optical transition radiation (OTR)[20] produced by the electron beam as it traverses a 25 μm thick titanium radiator placed at 45° with respect to the beam axis. Typical experimental data are shown in Fig. 5 where the plasma density is increased from 0 to 6×10^{14} cm^{-3}. The spot size of the beam is seen to oscillate at approximately twice the betatron frequency as expected. The beam envelope equation (solid line in Fig. 5) predicts the densities where the spot size minima and the spot size maxima occur up to a density of $\sim3\times10^{14}$ cm^{-3}. Beyond this, the beam is too long ($k_p\sigma_z < \sqrt{2}$) and n_{bo} becomes comparable to n_p. Therefore, the beam behavior is not well described by the envelope equation [Eq. (14)] where the focusing force is due to a pure ion channel.

In addition to the multiple oscillations of the overall beam envelope which occurs when an unmatched beam is sent into a plasma, the beam centroid (or center-of-mass of the beam) can also oscillate about the ion channel axis but at half the frequency of the envelope oscillation frequency. These centroid oscillations occur because the U-REB from a linear accelerator typically has a head-to-tail transverse tilt. The axis of the ion channel is defined by the head of the beam. This means that the bulk of the beam charge has an initial transverse offset with respect to the axis of the ion channel. This causes the beam centroid to oscillate about the axis at the betatron frequency. This oscillation can be quantified by measuring the position of the beam centroid downstream of the plasma using the OTR diagnostic. We have clearly observed these oscillations in our experiments [see Fig. 5(b)]. Again, the simple theory [Eq. (14)] with $\varepsilon_N = 0$ is able to predict the values of the plasma density where the beam returns to its original undeflected position as well as the actual magnitude of the deflection fairly well.

We have also plotted the exit angle σ' of the beam as a function of plasma density measured from the beam trajectory using 3 BPMs placed downstream of the plasma. This is shown in Fig. 6. One can see that the magnitude of the maximum exit angle scales as k_β or $\sqrt{n_p}$, Eq. (15) as manifested by sloshing of the bulk of the electrons in the ion channel.

D. The electron hosing instability

The transverse effects discussed so far are all zeroth order effects. Even though the electron beam is typically a few c/ω_p long, there is one transverse instability that is of concern to the stable propagation of the electron beam: the electron hosing instability.[21] The electron housing instability can lead to the growth of transverse perturbations on the beam due to the nonlinear coupling of the beam electrons to the plasma electrons at the edge of the ion channel through which the beam propagates.[21–23] As a result of this coupling these perturbations can grow nonlinearly leading to, in the worst scenario, the transverse break-up of the beam.

The differential equations that describe the coupling between the centroid offset of the beam slice x_b and the centroid offset of the preformed ion channel x_c at a position ξ within the beam are

$$\partial^2 x_b + k_\beta^2 x_b = k_\beta^2 x_c ,$$

$$\partial^2 x_c + \omega_0^2 x_c = \omega_0^2 x_b , \tag{17}$$

where $\xi = z/c - t$, $s = z$ and $\omega_0 = \omega_p/\sqrt{2}$. These equations can be numerically solved to calculate the growth of a particular beam slice at ξ after it has traversed a distance s in the plasma. However, in the asymptotic limit, the displacement $x_b(s,\xi)$ of the longitudinal slice of the beam with an initial linear head-to-tail tilt x_0 is given by[13]

$$x_b(s,\xi) = 0.341 \frac{x_0(\xi)}{A^{3/2}} e^A \cos\left\{ k_\beta s - \frac{A}{\sqrt{3}} + \frac{\pi}{12} \right\}, \tag{18}$$

where the factor

$$A = \frac{3^{3/2}}{4} [(k_\beta s)(\omega_0 \xi)^2]^{1/3}. \tag{19}$$

For beam parameters given in Table I, Eq. (18) predicts that there can be a factor 6 growth of a slice placed at $\xi = 5$ ps as it propagates through a meter long, 2×10^{14} cm^{-3} density plasma.

The above estimates raise a serious issue about the ability to propagate U-REB over long distances in dense plasmas. However, it should be noted that the theory assumes that a pre-formed channel with a constant radius exists whereas in many experimental situations the dynamically formed ion channel has a longitudinally varying radius. The theory also neglects longitudinal dynamics (see later) of the plasma electrons and nonideal experimental factors such as asymmetric beams and longitudinal density gradients. All these factors tend to suppress the hosing growth.

Using OSIRIS[24] we have carried out 3D, one-to-one PIC code simulations to study hosing when an U-REB propagates through long dense plasmas.[25] The physical dimensions of the system were $(17.6 \times 4 \times 4) c/\omega_p$ at a density of 1.7×10^{14} cm^{-3}. The beam had a Gaussian shape with $\sigma_z = 0.63$ mm, $\sigma_r = 40$ μm, $\varepsilon_N = 15$ mm-mrad, $Q = 3.4$ nC, and $\gamma = 6 \times 10^4$. These parameters are very close to the experimental beam parameters of Table III. The initial tilt on the beam was modeled using experimental data[25] as shown in Fig. 7(a). Figure 7(b) shows oscillations of two slices of the beam inside the plasma. The dotted line is the transverse motion of a 0.1 ps wide slice at the center of the beam. The bold line is the oscillation of a second 0.1 ps wide slice 5 ps behind the center slice. The dashed line is the behavior of the same slice obtained from numerical integration of Eq. (17) which predicts a growth factor of about 5 after 1.2 m propagation through the plasma. There appears to be some amplification of the offset of the slice at 5 ps as the beam propagates through the plasma. However, the amplification factor is about half of the theoreically predicted growth (dashed line).

Measurements are currently underway to check if this reduced growth rate seen in simulations indeed helps stable propagation of the electron beam in practice. These will be reported elsewhere.

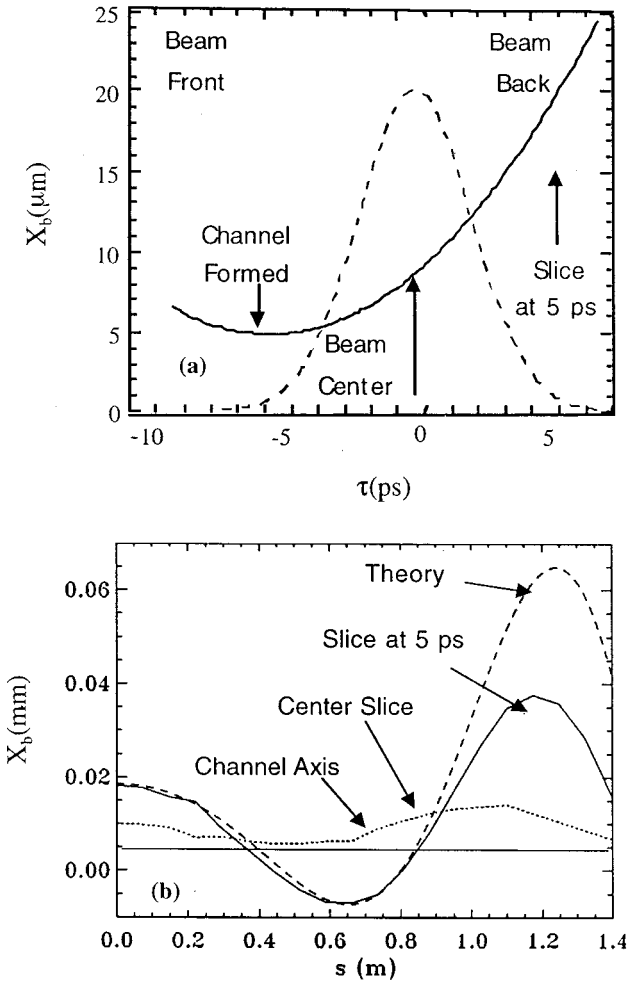

FIG. 7. (a) The longitudinal shape of the beam used in the OSIRIS simulations of electron housing. The axis of the ion channel is defined by $\tau = -5$ ps. (b) Results on growth of the transverse displacement of two slices of the beam due to the electron-hosing instability as the beam propagates through a 1.7×10^{14} cm^{-3}, 1.4 m long plasma using the 3D, PIC code OSIRIS. Also shown is the theoretically expected growth rate (dotted line) for the $\tau = 5$ ps slice using Eq. (18).

E. Emission of betatron radiation

There is a very important, observable consequence of betatron motion of electrons in a long ion column. It is the emission of betatron radiation in a narrow cone angle in the forward direction. This can be understood easily in the following way: Consider the motion of a single electron with an initial transverse displacement r_0 from the axis of the ion channel

$$\mathbf{r} = \mathbf{r}_0 \cos\phi,$$

$$\boldsymbol{\beta}_r = -\mathbf{r}_0 k_\beta \sin\phi, \tag{20}$$

$$\dot{\boldsymbol{\beta}}_r = -\mathbf{r}_0 k_\beta \omega_\beta \cos\phi \quad \text{with} \quad \frac{d\phi}{dt} = \omega_\beta .$$

As a result of this periodic acceleration the electron radiates betatron (synchrotron) radiation. The total radiation power is given by[26]

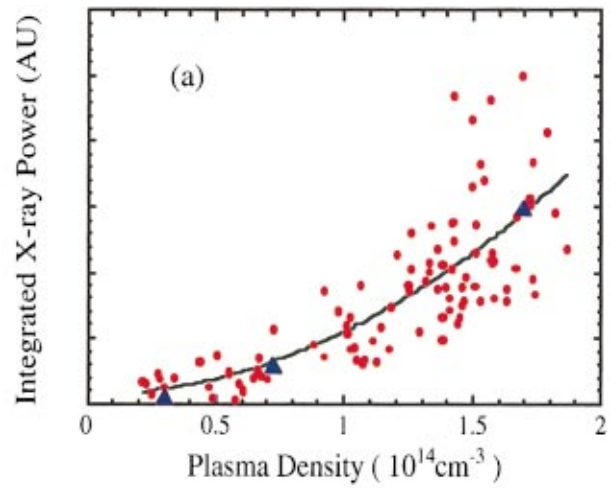

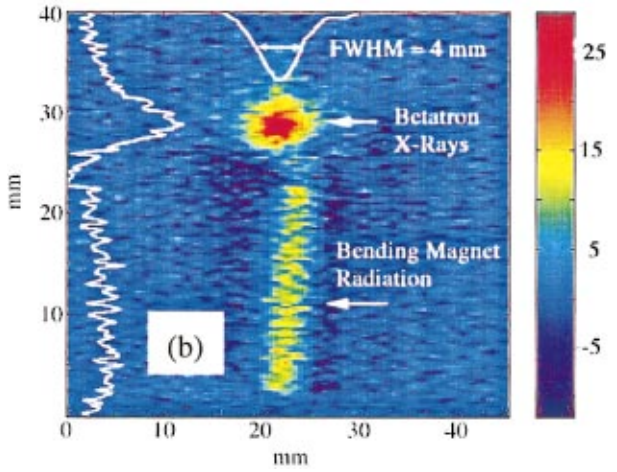

FIG. 8. (Color) (a) The estimated (triangles) and the measured (dots) x-ray energy in the 5–30 keV range as a function of plasma density. The solid line is a quadratic fit to the data. (b) Processed image produced on a fluorescent screen as recorded by a CCD camera showing the betatron x-rays produced by the plasma $n_p = 2\times10^{13}$ cm^{-3} (circle at the top) and a vertical stripe of remnant synchrotron radiation produced by a dipole bend magnet.

$$P(t) = \frac{2e^2\gamma^2}{3m^2c^3}[\dot{\mathbf{P}}^2 - m^2c^2\gamma^2] \cong \frac{2e^2\gamma^2\dot{\mathbf{P}}_r^2}{3m^2c^3}, \tag{21}$$

where $\mathbf{P}_r = \gamma mc\boldsymbol{\beta}_r$. Substituting for $\dot{\boldsymbol{\beta}}_r$ one can see that the total radiated power is proportional to ω_β^4 which scales as n_p^2. The radiation is emitted in a narrow cone angle in the direction of the propagation of the beam. This angle is $\sim\alpha/\gamma$ where α is the effective wiggler strength given by $\alpha = \gamma k_\beta r_0$ which for U-REB can be $\gg 1$. The spectrum of this betatron radiation has resonance frequencies[27] at

$$\omega_r = \frac{2m\gamma^2\omega_\beta}{[1+\alpha^2/2+(\gamma\Omega)^2]}, \tag{22}$$

where m is the harmonic number and $\Omega \ll 1$is the typical observation angle from the beam axis. In an electron beam, each electron has a different r_0 and, therefore, α which leads to broadening of the spectrum. The rate at which a single electron loses energy due to radiation is simply $\langle P\rangle/c$. Substituting for $\mathbf{P}_r$ and averaging over one betatron period one obtains

$$W_{\text{loss}} = \frac{\langle P\rangle}{c} = \frac{1}{3}r_e mc^2\gamma^2 k_\beta^2\alpha^2. \tag{23}$$

We have observed x-ray emission due to this betatron motion in our experiments where the beam excuses 1.5 betatron oscillations or 3 oscillations of its envelope.[28] Figure 8(a) shows the total radiated x-ray energy in the 5–30 keV range measured in a cone angle of roughly 10^{-4} radian in the forward direction approximately 40 meters from the exit of the plasma. One can see that the total energy increases as n_p^2 in reasonable agreement with theory. Figure 8(b) shows visible light image produced on a fluorescent paper by the x-rays emitted by the betatron motion (circle at the top) as well by the bending magnet that is used to separate the electron beam from the x-ray photons (the rectangular strip). From the size of the image ($\sim$4 mm FWHM) one can deduce the divergence angle of the betatron x-rays to be $\sim 10^{-4}$ radian. From the absolute number of x-ray photons at 14.2 KeV measured by precisely tuning the reflecting Si(111) crystal at the Bragg angle we have determined the brightness to be close to 8×10^{18} photons/s/mm^2/sr/0.1% bandwidth.

F. Acceleration and deceleration of beam particles

Now we come to the longitudinal phenomena. In expelling the plasma electrons to form an ion channel, the beam electrons do work and, therefore, must lose energy. If the beam is about half a plasma wavelength long the expelled electrons rush back in and set-up a plasma oscillation which has a longitudinal electric field given by[29]

$$eE = \sqrt{n_p}(\text{eV/m})\times\frac{n_b}{n_p}\sqrt{2\pi}k_p\sigma_z\frac{e^{-k_p^2\sigma_z^2}}{1+1/k_p^2\sigma_r^2}\sin k_p(z-ct). \tag{24}$$

For $k_p\sigma_z \cong \sqrt{2}$, an optimum wake field is excited. The above expression can be simplified in the limit when $eE/m\omega_p c \ll 1$ to

$$(eE)_{\text{linear}} = 240(\text{MeV/m})\left(\frac{N}{4\times10^{10}}\right)\left(\frac{0.6\,\text{mm}}{\sigma_z}\right)^2. \tag{25}$$

This is the so-called linear theory[30,31] result which predicts that the longitudinal peak accelerating field scales as $1/\sigma_z^2$ or the beam current divided by the bunch length.

When $n_b > n_p$, the linear theory is no longer valid and one has to resort to particle-in-cell (PIC) code simulations to determine the exact shape and magnitude of the nonlinear wake induced by short, high-current bunches in a plasma.[29] Figure 9 shows an example of such a wake using the code OSIRIS for a $\sigma_z = 100$ μm beam containing 2×10^{10} electrons focused to a 20 μm spot size in a 5.6×10^{15} cm^{-3} plasma. For these parameters the $(eE)_{\text{linear}}$ should be 4.32 GeV/m. Since in the linear theory, the transformer ratio, defined as the ratio of the accelerating field to the decelerating field, is always 2 for a symmetric bunch, the drive bunch slows down at a rate 2.16 GeV/m. The simulations show that

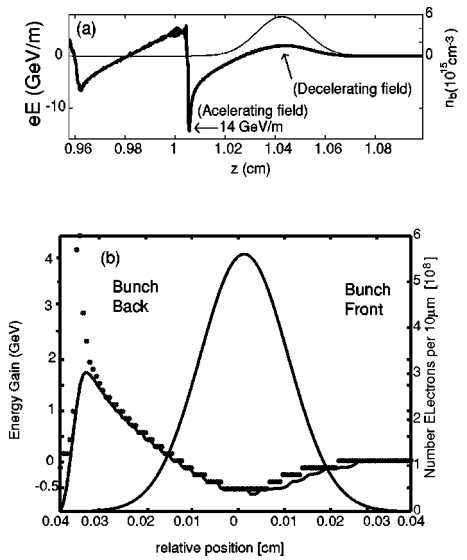

FIG. 9. (a) On axis longitudinal accelerating–decelerating field induced by a $\sigma_z=0.1$ mm long electron bunch containing 2×10^{10} particles, $\gamma=60\ 000$ in a 5.6×10^{15} cm^{-3} plasma $\varepsilon_N=50$ mm-mrad and $\sigma_r=20$ μm. (b) The energy change of the different longitudinal 10 μm long slices of the electron beam (a) after traversing a 30 cm length of the plasma. The largest average energy gain is 1.75 GeV, but some particles gained up to 4.4 GeV. Both (a) and (b) are from 3D, OSIRIS, PIC simulations.

the wake is highly nonlinear with the longitudinal field having a large accelerating spike on axis where the plasma electrons that are expelled by the beam all rush back in to set-up large density spike. The decelerating field is 1.8 GeV/m whereas the peak accelerating field is >14 GeV/m giving a transformer ratio of >7. In the nonlinear regime the wavelength of the plasma wake is reduced and consequently the optimum plasma density is higher than that predicted by the linear theory.

Figure 9(b) shows the energy change that occurs to different longitudinal slices of the beam after traversing just 30 cm of the dense plasma. The bulk of the electrons lose approximately 600 MeV energy whereas the average energy gain of a beam slice approximately 1.2 ps behind the center of the bunch is 1.75 GeV with some particles gaining as much as 4.4 GeV. This simulation shows the potential for achieving extraordinarily high gradients in beam-driven wake field acceleration [known as the plasma wake field acceleration scheme (PWFA)] that were previously thought only possible using intense laser beams interacting with a dense plasma. As we have shown, because it is possible to propagate electron bunches over meter long distances, prospects for obtaining large energy gains using an U-REB driver are extremely likely. In fact, beam and plasma parameters used in the above simulation form the basis of a recently approved PWFA experiment at SLAC known as E164.

Interestingly, even the peak accelerating gradient in this highly nonlinear regime still seems to follow the $1/\sigma_z^2$ scaling law. In Fig. 10 for instance, the 3D PIC simulation result for a $\sigma_z=40$ μm bunch shows a peak gradient of greater than 40 GeV/m. Such short bunches containing 2×10^{10} electrons have recently become realizable. In fact, the proposed Ultrashort Bunch Facility at SLAC[32] will generate electron

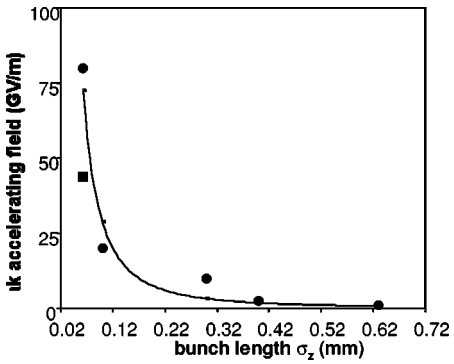

FIG. 10. The peak accelerating field vs the bunch length from PIC simulations and a $1/\sigma_z^2$ fit to the simulations.

bunches that are as short as 30 fs ($\sigma_z=10$ μm) within a year. Such short bunches lead to extremely high gradients and make feasible an energy doubler[33] experiment using a 50 GeV driver whereby the drive bunch is nearly depleted of its energy in a column of plasma that is just a few meters long while a trailing bunch is accelerated to about twice the drive bunch energy. The issues of emittance preservation and energy spread are being addressed through calculations and simulations for such an ''afterburner'' for a conventional linear collider.

It should be remarked that wakes generated by an electron beam can also be used to accelerate positrons[34] and muons (μ^+,μ^-). Similarly, the wakes themselves can be produced using positively charged particles although the physics of wake excitation is qualitatively different. As an example consider positron beam induced wakes. When a positron beam enters a quasi-neutral plasma, it attracts plasma electrons from a region that is $\sim c/\omega_p$ wide instead of expelling them as an electron drive bunch would do. There is a spread in the arrival time of these electrons that are being ''pulled-in'' on axis since they originate at different radii. This phase mixing leads to a lower longitudinal field being excited in the case of a positron driver compared to when an electron bunch is used. Figure 11 compares positron and electron beam excited wakes for identical drive beam parameters which demonstrates this effect. It has been suggested that a positron beam propagating in a hollow channel that is roughly c/ω_p in diameter would lead to an increase in

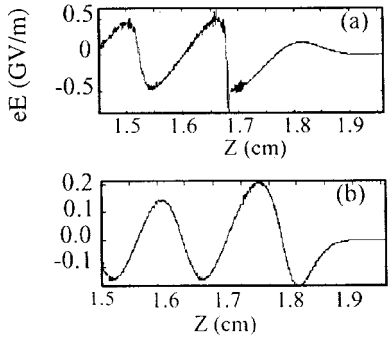

FIG. 11. Comparison of the electron (a) and positron (b) wakes produced in a plasma. $N=2\times10^{10}$, $\sigma_z=0.4$ mm, $\sigma_r=75$ μm, $n_p=4.3\times10^{14}$ cm^{-3}. The beams are propagating from the left to the right.

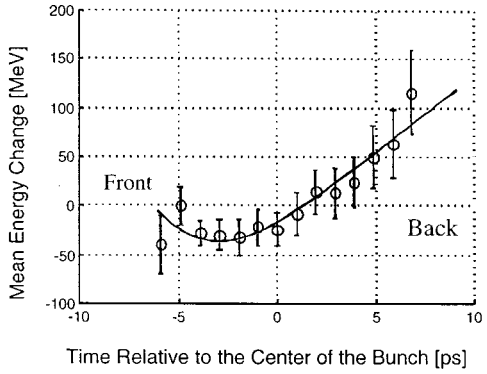

FIG. 12. A slice-by-slice analysis of the centroid of 1 ps beam slices, showing an indication of energy loss for bulk of the beam and energy gain by the tail particles in the beam.

eE because the positron beam would pull-in electrons from the wall of the channel. Since the electrons now originate at the same radius, their arrival time on axis is the same leading to a larger accelerating gradient.

In the experiments we have studied the energy loss and gain of the beam particles due to the longitudinal dynamics in the plasma using parameters shown in Table III. Time resolved energy spectra were obtained from streak camera images of the beam in the dispersive plane (see Fig. 1) after the FFTB bending magnet. The images are analyzed by slicing the streaks in 1 ps time slices and then the centroid energy of each slice is calculated. Analysis of a typical single event shown in Fig. 12 indicates that the core of the beam has lost about 50 MeV while the electrons in the last slice ($+7$ ps) have gained about 120 MeV. The plasma density for this event was close to the optimum density and the beam exited the plasma after 3 betatron oscillations at a plasma transparency point. It should be noted that because of the space-charge broadening in the streak camera the actual time of these accelerated electrons is somewhat earlier. [In the simulations the maximum energy gain occurs for $\tau = +5$ ps.] In this run an imaging spectrometer was not used to both disperse the electrons and image the exit of the plasma. Although there appeared to be no significant tail on the beam due to the head-to-tail tilt and the data was taken at a plasma transparency point, the streak camera data can be sensitive to transverse motion of the particles. However, we have recently obtained data from a reconfigured experimental set-up which uses an imaging spectrometer to confirm the energy loss of the core and energy gain of the back slices of the beam. The results show that under optimum conditions the beam core can lose up to 170 MeV energy while there is an energy gain exceeding 350 MeV in the tail. These results will be published elsewhere.

IV. CONCLUSIONS

HEDPS with an ultrarelativistic electron beam is seen to be a fertile research area of beam and plasma physics that is relatively unexplored. Some of the physical effects are steering (refraction), focusing, betatron oscillations, emission of spontaneous x-ray radiation due to the betatron motion, and acceleration and deceleration of the beam particles themselves. These phenomena can be theoretically predicted and are seen in full-scale PIC code simulations. There is a good agreement seen between experimental results and theory and simulations. There is promise that HEDPS with U-REBs will affect future accelerator and light source technologies.

ACKNOWLEDGMENTS

We thank J. M. Dawson, P. Raimondi, F. J. Decker, R. Iverson, P. Catravas, W. Leemans, E. Esarey, S. Chattopadhyay, D. Whittum, S. Rokni, and R. Assmann for their contributions to this work.

This work was supported by DOE Grants No. DE-AC03-76SF00515, No. DE-AS03-76SF0098, and No. DE-FG03-98DP0021, and NSF Grant No. ESC 9617089.

[1] E. M. Campbell and M. J. Hogan, Plasma Phys. Controlled Fusion **41**, 39 (1999); M. D. Rosen, Phys. Plasmas **3**, 1803 (1996).
[2] N. Barov, M. Conde, J. B. Rosenzweig, J. B. Schoessow, G. Cox, W. Gai, R. Konecny, J. Power, and J. Simpson, *Proceedings of 1995 Particle Accelerator Conference*, Dallas, TX (IEEE, Piscataway, NJ, 1996), p. 631; J. B. Rosenzweig, B. Briezman, T. Katsouleas, and J. J. Su, Phys. Rev. A **44**, R6189 (1991); T. Katsouleas, S. Wilks, P. Chen, J. M. Dawson, and J. J. Su, Part. Accel. **22**, 81 (1987).
[3] N. Barov, J. B. Rosenzweig, M. E. Conde, W. Gai, and J. G. Power, Phys. Rev. ST Accel. Beams **3**, 011301 (2000).
[4] N. Barov, M. E. Conde, W. Gai, and J. B. Rosenzweig, Phys. Rev. Lett. **80**, 81 (1998).
[5] G. Hairapetian, P. Davis, C. E. Clayton, C. Joshi, S. C. Hartman, and C. Pellegrini, Phys. Rev. Lett. **72**, 2403 (1994); G. Hairapetian, P. Davis, C. E. Clayton, C. Joshi, C. Pellegrini, and T. Katsouleas, Phys. Plasmas **2**, 2555 (1995).
[6] D. A. Hammer and N. Rostoker, Phys. Fluids **13**, 1831 (1970).
[7] M. Hogan, C. E. Clayton, P. Muggli, R. Siemann, and C. Joshi, Phys. Plasmas **7**, 2241 (2000).
[8] P. Muggli, K. A. Marsh, S. Wang, C. E. Clayton, S. Lee, T. C. Katsouleas, and C. Joshi, IEEE Trans. Plasma Sci. **27**, 791 (1999).
[9] P. Catravas, S. Chattopadhyay, E. Esarey *et al.*, Phys. Rev. E **64**, 046502 (2001).
[10] NRL Plasma Formulary, NRL/PV/6790-98-358.
[11] J. D. Lawson, *The Physics of Charged Particle Beams* (Oxford University Press, London, 1988).
[12] S. Humphris, *Charged Particle Beams* (Wiley, New York, 1990); J. L. Cox and W. H. Benett, Phys. Fluids **13**, 182 (1970); W. H. Benett, Phys. Rev. Lett. **45**, 890 (1934).
[13] D. H. Whittum, A. Sessler, and J. M. Dawson, Phys. Rev. Lett. **64**, 2511 (1990).
[14] A. Geraci and D. H. Whittum, Phys. Plasmas **7**, 2241 (2000).
[15] J. S. T. Ng, P. Chen, H. Baldis *et al.*, Phys. Rev. Lett. **87**, 244801 (2001).
[16] J. G. Davis, Ph.D. thesis, University of California, Los Angeles, 1996.
[17] J. B. Rosenzweig and P. Chen, Phys. Rev. D **39**, 2039 (1989).
[18] C. Huang, V. Decyk, S. Wang *et al.*, Bull. Am. Phys. Soc. **46**, 91 (2001).
[19] P. Muggli, S. Lee, T. Katsouleas *et al.*, Nature (London) **411**, 43 (2001); P. Muggli, S. Lee, T. Katsouleas *et al.*, Phys. Rev. ST Accel. Beams **4**, 091301 (2001).
[20] C. Clayton, B. E. Blue, E. S. Dodd *et al.*, "Transverse envelope dynamics of a 28.5 GeV electron beam in a long plasma," Phys. Rev. Lett. (in press).
[21] D. H. Whittum, W. Sharp, S. S. Yu, M. Lampe, and G. Joyce, Phys. Rev. Lett. **67**, 991 (1991).
[22] D. H. Whittum, M. Lampe, G. Joyce, S. P. Slinker, S. S. Yu, and W. M. Sharp, Phys. Rev. A **46**, 6684 (1992).
[23] M. Lampe, G. Joyce, S. P. Slinker, and D. H. Whittum, Phys. Fluids B **5**, 1888 (1993).
[24] K. C. Tzeng, W. B. Mori, and C. D. Decker, Phys. Rev. Lett. **76**, 3332 (1996).
[25] B. Blue, C. E. Clayton, E. Dodd *et al.*, "Test of the electron hose instability in the E157 experiment," *Proceedings of the 2001 Particle Accelerator Conference*, Chicago, IL (IEEE, Piscataway, NJ, in press).

[26]J. D. Jackson, *Classical Electrodynamics* (Wiley, New York, 1975).
[27]E. Esarey, P. Catravas, and W. P. Leemans, *Proceedings of the Advanced Accelerator Concepts 9th Workshop, Santa Fe, NM, 2000*, AIP Conf. Proc. No. 569, edited by P. L. Colestock and S. Kelley (American Institute of Physics, Melville, NY, 2001), p. 473.
[28]S. Wang, C. E. Clayton, B. E. Blue *et al.*, "X-ray emission from betatron motion in a plasma wiggler," Phys. Rev. Lett. (in press).
[29]S. Lee, T. Katsouleas, R. Hemker, and W. B. Mori, Phys. Rev. E **61**, 7014 (2000).
[30]T. Katsouleas, Phys. Rev. A **33**, 2056 (1986).
[31]T. Katsouleas, S. Wilks, P. Chen, J. M. Dawson, and J. J. Su, Part. Accel. **22**, 81 (1987).
[32]P. Emma, R. Iverson, P. Krejcik, P. Raimondi, and J. Safranek, "Femtosecond electron bunch lengths in the SLAC FFTB beamline," *Proceedingsof the 2001 Particle Accelerator Conference*, Chicago, IL (IEEE, Piscataway, NJ, in press).
[33]S. Lee, T. Katsouleas, P. Muggli *et al.*, Phys. Rev. ST Accel. Beams **5**, 011001 (2002).
[34]S. Lee, T. Katsouleas, R. G. Hemker, E. S. Dodd, and W. B. Mori, Phys. Rev. E **64**, 045501 (2001).

Appendix C

Betatron Radiation Induced Positron Source For a Linear e^+-e^- Collider

C. Joshi

INTRODUCTION

The E164 experiment at SLAC is designed to use 100 μm long bunches to generate accelerating gradients exceeding 1 GeV/m in a plasma [i]. This experiment and its follow on experiment (E-164X) presents an opportunity to explore yet another possible application of plasmas to future e^+e^- colliders: Positron Production. An efficient method of generating positrons that does not have survivability problems is needed for the NLC and other future e^+e^- colliders. Here we propose to explore betatron radiation induced positron source as an alternative to the bremstrahlung induced pair-production for a future collider. Our method is particularly attractive because the electron beam only interacts with a plasma, removing the heating/cracking problem faced by a solid target.[ii] The beam is then defocused rapidly as it exits the plasma whereas the betatron x-rays which diverge as K/γ interact with a high-Z target where they are attenuated by pair production. We estimate that with the beam parameters available at the FFTB (see Table 1) it should be possible to generate several positrons per electron in a meter long plasma that will ultimately escape the target.

Here we are proposing to test this idea by using a much shorter plasma section, approximately 10 cm in length, to avoid the beam dumping issue associated with a meter long plasma.

PAIR PRODUCTION FROM BETATRON X-RAYS

Table 1 gives the electron beam parameters that should be available at the FFTB in the near future using the Ultra Short Beam Facility (USBF)[iii].

TABLE 1. USBF parameters at IPO of the FFTB at SLAC.

Energy (GeV)	28.5
Energy Spread (r.m.s.)	1.5%
Pulse Width σ_z (μm)	20-100 μm
Beam Radius σ_z (μm)	10-25 μm
N	1-2 $\times$ 10^{10}

The E157 experiment showed that an unmatched electron beam undergoes betatron oscillations in the plasma [iv]. The focusing force, in the underdense limit $n_b > n_p$ is given by

$$E_r\,(\mathrm{MV/m}) = 9 \times 10^{-15}\, n_p\,(\mathrm{cm^{-3}})\, r\,(\mu\mathrm{m})\, r \Gamma 1.5\, \sigma_r \qquad (1)$$

where σ_r is the radial spot size of the beam. As a consequence of these oscillations electrons emit photons[v]. The frequency of radiation emitted by a single electron is $\omega_m = 2\gamma^2 m \omega_\beta / (1 + K^2/2)^{1/2}$ where $K = \gamma k_\beta r_o$ is the betatron strength parameters and r_o is the displacement of the electron from the axis of the ion channel. Because different electrons in an actual beam have different r_o the overall spectrum tends to smear out and resemble the bending magnet spectrum with a critical frequency given by

$$\omega_c = 2\gamma^3 c/2\rho$$

where ρ is the radus of curvature of the motion. A handy formula for ω_c is

$$(\hbar\omega_c)(\mathrm{MeV}) = 2 \times 10^{-4}\, (E/\mathrm{GeV})^2 \left(n_p/10^{15}\mathrm{cm^{-3}}\right)\left(r/\mu\mathrm{m}\right) \qquad (2)$$

In order that the underdense expressions above are valid for the E-164X parameters we take $N = 2 \times 10^{10}$ particles in a $\sigma_z = 20$ μm, $\sigma_r = 20$ μm giving $n_b = 8 \times 10^{16}$ $\mathrm{cm^{-3}}$. Thus for $\gamma = 5.6 \times 10^4$ the critical frequency is 260 MeV. This is far above the e^+-e^- pair creation threshold [vi].

The energy loss rate to the radiation field by a single electron is given by

$$\frac{\partial w}{\partial z} = r_e m_e c^2 \gamma^2 k_\beta^2 K^2 / 3 \qquad (3)$$

which scales as $\sim n_p^2 \gamma^2 r_o^2$. For E-164X parameters $\frac{\partial w}{\partial z}$ = 1.28 GeV/m. The proposed length of the plasma in E-164X is 10 cm giving an average energy loss per electron through betatron radiation of 128 MeV almost all of which appears in photons above the

1 MeV e^+e^- threshold energy. Assuming an average photon energy of $\hbar\omega_c / 2$ MeV, each electron radiates about 1 photon in a roughly K/γ angle in the forward direction.

On the other hand, an electron that is only 2 μm away from the axis of propagation will emit x-rays with a critical frequency of 26 MeV with an average energy loss of 1.28 MeV. . (i.e., about 10 electrons are needed to emit one photon.) Clearly, electrons with r << μm do not contribute to $(\hbar\omega)_{x\text{-}rays} > 1$ MeV that is needed to produce e^+-e^- pairs. However, even in a Guassian beam with $\sigma_r = 20$ μm, most of the electrons reside between μm < r < σ_r.

As mentioned above, the rough divergence angle is K/γ which for <r> = 10 μm turns out to be ~ 14 mrad. Thus after 50 meters of propagation through the photon beam line the x-ray spot size will be 75 cm in diameter. If we intercept about 2 cm aperture at the center of this x-ray beam we intercept about $(2/75)^2 \approx 7 \times 10^{-4}$ of the x-ray flux.

Thus, of the estimated 2×10^9 photons with an average energy of 50 MeV, 1.4×10^6 will strike the 2 cm diameter, 5 mm thick high-Z target where they are attenuated via the pair-production [vii] mechanism. Assuming the attenuation coefficient μ = 1.3 cm-1 roughly 50% of the x-ray photon will be converted into pairs, i.e. $> 7 \times 10^5$, with positron energy going from a few MeV to about 100 MeV. We have an imaging magnetic spectrometer in this energy range which can accept this cone angle and capture all the particles entering it. In the spectrometer the electrons are bent one way while the positrons are bent the other way. The detection will be done using 1 mm thick Silicon-surface barrier detection which measure the charge induced in the detectors as the particles traverse through.

CONCLUSIONS

As can be seen from the above estimates, the beam parameters needed for demonstrating plasma production via tunneling ionization in the E-164X experiment are nearly identical to those needed for the pair-production from betatron radiation experiment. In fact, the beam quality needed to copiously produce positrons need not be very high. The head of the beam will define the channel axis. Both the oscillations of the beam envelope and the tail will produce betatron x-rays. We feel that this is a worthwhile experiment to do that in its own right that could impact high energy physics.

We thank Dr. Sho Wang of UCLA and Dr. Rainer Pitthan of SLAC for useful discussions at the AAC '02 Workshop. This work is supported by DOE grant number DE-AS03-92ER40727.

[i] M.J. Hogan et al., SLAC-ARDB-314 (2000).
[ii] F. Bulos et al., *IEEE Trans. Nucl. Sc.* **NS-32**, 1832 (1985).
[iii] P. Emma et al., SLAC-PUB-8850 (2001).
[iv] C.E. Clayton et al., *Phys. Rev. Lett.* **88**, 154801 (2002).
[v] S. Wang et al., *Phys. Rev. Lett.* **88**, 135004 (2002).
[vi] W. Heitler *The Quantum Theory of Radiation*, Oxford University Press (1960).
[vii] Eisberg, R., *Review of Modern Physics*, John Wiley and Sons, N.Y. (1961).